

More on Dimension-4 Proton Decay Problem in F-theory — Spectral Surface, Discriminant Locus and Monodromy —

Hiroataka Hayashi¹, Teruhiko Kawano¹, Yoichi Tsuchiya¹ and Taizan Watari²

¹*Department of Physics, University of Tokyo, Tokyo 113-0033, Japan*

²*Institute for the Physics and Mathematics of the Universe, University of Tokyo,
Kashiwanoha 5-1-5, 277-8583, Japan*

Abstract

Factorized spectral surface scenario has been considered as one of solutions to the dimension-4 proton decay problem in supersymmetric compactifications of F-theory. It has been formulated in language of gauge theory on 7+1 dimensions, but the gauge theories descriptions can capture physics of geometry of F-theory compactification only approximately at best. Given the severe constraint on the renormalizable couplings that lead to proton decay, it is worth studying without an approximation whether or not the proton decay operators are removed completely in this scenario. We clarify how the behavior of spectral surface and discriminant locus are related, study monodromy of 2-cycles in a Calabi–Yau 4-fold geometry, and find that the proton decay operators are likely to be generated in a simple factorization limit of the spectral surface. A list of loopholes in this study, and hence a list of chances to save the factorized spectral surface scenario, is also presented.

1 Introduction

Considerable progress has been made in the last two years in understanding flavor structure in F-theory compactifications. Supersymmetric compactifications of F-theory to 3+1 dimensional space-time is described primarily by a set of data $(X_4, G^{(4)})$, where X_4 is an elliptic fibered Calabi–Yau 4-fold and $G^{(4)}$ a 4-form flux on it. Non-Abelian gauge theories like $SU(5)_{\text{GUT}}$ unified theories can arise from singular geometry of X_4 . It is difficult to extract physics directly from singular geometry, but low-energy effective theory associated with the singular local geometry of X_4 can be described by using non-Abelian gauge theory in 7+1 dimensions [1] to some level of approximation. It has been the key in the progress in the understanding of flavor structure in F-theory to use this gauge-theory effective description [2, 3]. See also [4, 5, 6, 7, 8, 9].

In supersymmetric compactification for realistic models, dimension-4 proton decay operators

$$\Delta W \ni \bar{\mathbf{5}}_M \cdot \mathbf{10} \cdot \bar{\mathbf{5}}_M \quad (1)$$

have to be brought under control. An obvious solution is

- (i) to consider a compactification with $(X_4, G^{(4)})$ that has a \mathbb{Z}_2 symmetry [6].

The \mathbb{Z}_2 symmetry will become an R -parity (or equivalently a matter parity) in the low-energy effective theory below the Kaluza–Klein scale. Other solutions to the problem include

- (ii) rank-5 GUT scenario, that is, to consider $SU(6)$ or $SO(10)$ GUT models [10],
- (iii) factorized spectral surface scenario [6, 11] (see also [12, 13, 14, 15]), and
- (iv) spontaneous R -parity violation scenario [10, 6] (see also [16]).

The scenario (ii) is a special case of (iii), and is also a special case of (iv).

The factorized spectral surface scenario (iii), however, is not without a theoretical concern [6]. The dimension-4 proton decay problem is so severe that the coupling (1) should be extremely small even if they are present. The question is whether we have a theoretical framework in which the scenario can be formulated rigorously and even an extremely small contribution to (1) can be studied. At least so far, the answer is no. It is, thus, important to study to what extent this scenario works, and that is what we do in this article.

Heart of the idea of the factorized spectral surface scenario is to consider a factorization limit of the spectral surface so that

- matter fields $\bar{\mathbf{5}}_M$ and Higgs fields $\bar{\mathbf{5}}_H$ are associated with irreducible components of the spectral surface for fields in the $\bar{\mathbf{5}}$ representation of $SU(5)_{\text{GUT}}$, and
- an unbroken $U(1)$ symmetry remains in the low-energy effective theory below the Kaluza–Klein scale, and the operator (1) is ruled out because of the symmetry.

This scenario has been formulated by using the gauge theory description in 7+1 dimensions. Because of the approximate nature of the gauge theory description, factorization is not rigorously well-defined; there are also some corrections that have not been captured in the gauge theory description on 7+1 dimensions [6]. We will explain these limitations of the gauge theory description on 7+1 dimensions more in detail in section 2, although these materials have almost been spelled out in [6, 11] (see also [5]).

In section 3, we study monodromy of 2-cycles in X_4 instead of a gauge theory on 7+1 dimensions, in order to find out whether an unbroken $U(1)$ symmetry remains in the low-energy effective theory. We conclude in section 4 that the proton decay operators (1) are expected to be generated in the factorized spectral surface scenario, but we also list some loopholes in the argument. The appendix A explains calculation of the monodromy of 2-cycles using language of string junction in detail; all the necessary techniques in the appendix A, however, are already available in the literature (e.g., [17]). The monodromy matrices obtained in this way in F-theory language can be understood much more transparently in dual Heterotic language; this is the subject of the appendix B.

2 Effects Beyond Gauge Theory in 7+1 Dimension

The gauge theory description on 7+1 dimensions in F-theory captures geometry of a local neighbourhood of a discriminant locus of an elliptic fibration [1]. When a geometry of an elliptically fibered Calabi–Yau 4-fold $\pi_X : X_4 \rightarrow B_3$ is locally approximately an ALE space of A–D–E type in the direction transverse to the discriminant locus, gauge theory of the same A–D–E type describes the physics associated with this local geometry. Thus, by construction, the gauge theory description has limited power in capturing the physics of geometry in the transverse direction; only physics associated with *non-compact* (local) geometry that is *approximately* ALE fibration can be captured *approximately*. When it comes to the dimension-4 proton decay problem, this approximate nature of the gauge theory description of F-theory can be a problem.

To see this more explicitly, let us consider a local geometry given by the generalized

Weierstrass form

$$y^2 = x^3 - A_1 yx + A_2 x^2 - A_3 y + A_4 x + A_6, \quad (2)$$

where (x, y) are coordinates of the elliptic fiber of X_4 , and $A_{1,\dots,4,6}$ are regarded as functions locally on B_3 . For an $SU(5)_{\text{GUT}}$ GUT model [18], we need to consider a case where $A_{1,\dots,4,6}$ are in the form of

$$A_k = (-)^k [z^{k-1} a_{6-k} + z^k a'_{6-k} + z^{k+1} a''_{6-k} + \dots], \quad (3)$$

where z is a local coordinate of a base manifold B_3 ; the $z = 0$ locus becomes an irreducible component S_{GUT} of the discriminant locus Δ . $a_{0,2,3,4,5}$ and $a'_{0,2,3,4,5}$ are coefficients that depend on two local coordinates on S_{GUT} . Consider, for example, a case^{1,2} when all of $a_{2,3,4,5}$ are small in a way indicated by

$$a_5 = \epsilon_K^5 a_{5,*}, \quad a_4 = \epsilon_K^4 a_{4,*}, \quad a_3 = \epsilon_K^3 a_{3,*}, \quad a_2 = \epsilon_K^2 a_{2,*} \quad (5)$$

for $a_{5,*}, a_{4,*}, a_{3,*}, a_{2,*}$ of all $\sim \mathcal{O}(1)$. ϵ_K is a small parameter that is different from zero. We know that this geometry nearly has an E_8 singularity around $z = 0$; to be more precise, there are four vanishing 2-cycles right at $z = 0$, and there are four small 2-cycles near $z = 0$. One can focus on the geometry of these small 2-cycles by choosing a new set of coordinates (x', y', z') :

$$x = \epsilon_K^{10} x', \quad y = \epsilon_K^{15} y', \quad z = \epsilon_K^6 z'. \quad (6)$$

With these new coordinates and coefficients $a_{r,*} \sim \mathcal{O}(1)$ ($r = 0, 2, 3, 4, 5$), the local defining equation (2) becomes exactly the E_8 singularity with relevant deformation parameters [19], with correction terms whose coefficients are suppressed by positive power of the small number ϵ_K . The gauge theory description focuses on the geometry of these small 2-cycles (i.e., forgets about the rest of the geometry), and further make an approximation of ignoring the correction terms that are small but present [4] (see also [5, 11]). Even when the ϵ_K scaling

¹This can be interpreted as considering a region of S_{GUT} where the condition (5) is satisfied.

² Additional scaling may hold in some regions of S_{GUT} . For example, along the matter curve $a_5 = 0$,

$$a_{5,*} = \lambda \tilde{a}_{5,*}, \quad \tilde{a}_{5,*} \sim \mathcal{O}(1) \quad (4)$$

is satisfied for $\lambda \ll 1$. One of the four 2-cycles corresponding to the simple roots of the structure group $SU(5)_{\text{str}}$ becomes much smaller than all the others in this region, and this corresponds to a hierarchical symmetry breaking $E_8 \rightarrow D_5 \rightarrow A_4$. The rank-1 extended gauge theories in [1] and rank-2 extended gauge theories in [3, 4] describe physics of local geometries that have such scalings. We also introduce a hierarchical symmetry breaking in the choice of a base point of monodromy analysis in (19) in this article.

of the coefficients is assumed as above to maximize the number of small 2-cycles captured in a gauge theory description, the gauge theory description is only an approximate description of the compact geometry X_4 by construction [6]. Let us call this **Problem A**.

We may have another difficulty in justifying the factorized spectral surface scenario in the gauge theory description. To see this, let us remind ourselves of the following. Since $\bar{\mathbf{5}}_M$ and $\bar{\mathbf{5}}_H$ multiplets are zero modes appearing in the low-energy effective theory below the Kaluza–Klein scale, the factorization of the spectral surface should be defined *globally* on the GUT divisor S_{GUT} . Field theory local model in an open patch $U_a \subset S_{GUT}$, on the other hand, captures very small 2-cycles in the ALE fiber in addition to the four vanishing 2-cycles in A_4 singularity, and hence the rank of gauge group in U_a may be different from the rank in another open patch $U_b \subset S_{GUT}$ [1, 3, 13, 4]; these local descriptions with gauge groups of varying rank are glued together approximately in overlapping regions of open patches $\{U_a\}_{a \in A}$ to cover the entire ALE-fibered geometry over S_{GUT} . The global factorization of the spectral surface, however, cannot be well-defined, when the rank of the spectral surface varies from one patch to another. This problem can be avoided if we consider a Higgs bundle that has a fixed rank over the entire S_{GUT} .

Fixed rank Higgs bundle description over the entire S_{GUT} , however, often breaks down somewhere in S_{GUT} . For example, a rank- k spectral surface C is defined globally in K_S by

$$a_{5-k}\xi^k + \cdots + a_4\xi + a_5 = 0, \quad (7)$$

where ξ is the fiber coordinate of the canonical bundle $\pi_{K_S} : K_S \rightarrow S$, if a_r 's ($5-k \leq r \leq 5$) are global holomorphic sections of line bundles $\mathcal{O}(rK_S + \eta)$ for some divisor η in S_{GUT} . $\pi_{K_S}|_C : C \rightarrow S$ is an k -fold cover at generic points of S_{GUT} , but when the coefficient of the highest degree term a_{5-k} vanishes, one of the k solutions of (7) shoots off to infinity in the fiber direction of $\pi_{K_S} : K_S \rightarrow S_{GUT}$. This behavior of the spectral surface indicates that one of (very) small 2-cycles becomes relatively large there.³ It is not a sensible approximation to keep the physics associated with all the 2-cycles in (7) while ignoring all others in a local neighbourhood around the zero locus of a_{5-k} . As long as the divisor $(5-k)K_S + \eta$ is effective,⁴ this does happen somewhere in S_{GUT} . The problem in this neighbourhood can

³ The vev of the Higgs field φ is obtained by a holomorphic 4-form on a Calabi–Yau 4-fold on 2-cycles. The φ vev being large means that the period integral over the corresponding 2-cycle is large [2, 6].

⁴ The divisor $5K_S + \eta$ needs to be effective so that the matter curve for the $\text{SU}(5)_{\text{GUT-10}}$ representation field is effective. If $-K_S$ is effective, as in del Pezzo surfaces and Hirzebruch surfaces, then $(5-k)K_S + \eta$ is also effective. Thus, this problem is unavoidable for surfaces S_{GUT} with effective $-K_S$. See section 4 for comments on S_{GUT} with effective K_S (rather than effective $-K_S$).

be fixed (c.f. [3]) by adopting a Higgs bundle that is one-rank higher, a rank- $(k+1)$ Higgs bundle, as long as a_{4-k} is not identically zero.⁵ We still encounter the same problem around the zero locus of a_{4-k} . One could still crank the rank of gauge group up, once again. But E_8 gauge group is maximal in the E series of the A–D–E classification, and we come to a dead end.

We could consider a Calabi–Yau 4-fold X_4 for F-theory compactification which is approximately an ALE fibration of E_8 type over S_{GUT} in the neighbourhood along S_{GUT} . This is done by choosing the coefficients indicated as in (5) [5]. When we take GUT gauge group as $SU(5)_{GUT}$, we have a 5-fold spectral cover,

$$a_0\xi^5 + a_2\xi^3 + a_3\xi^2 + a_4\xi + a_5 = 0. \quad (8)$$

Factorization conditions can be imposed on (8) in an E_8 gauge theory defined globally on S_{GUT} [11]. That is the best we hope to do within gauge theories on 7+1 dimensions. In a region of S_{GUT} around a point where a_0 vanishes, however, two roots of (8) become large, as

$$\xi \sim \pm i\sqrt{(a_2/a_0)}. \quad (9)$$

The E_8 gauge theory is not a sensible approximation in the local neighbourhood of the $a_0 = 0$ locus, because the corresponding two 2-cycles are no longer relatively small. In a region slightly away from the $a_0 = 0$ locus, one can see that the two roots (and hence the Higgs field vevs φ in two diagonal entries) are exchanged when the phase of a_0 changes by 2π . This phenomenon indicates that the two 2-cycles not just become large, but also are twisted by a monodromy around the $a_0 = 0$ locus. 2-cycles that are not captured by the E_8 gauge theory may also be involved in this monodromy, because there is no clear separation between the 2-cycles within E_8 and those that are not around the $a_0 = 0$ locus. In order to study geometry and physical consequences associated with this behavior, one has to go beyond E_8 gauge theory on 7+1 dimensions. We call this **Problem B**.

Clearly we need a theoretical idea how to study whether the operator (1) is generated or not; a new idea should keep the successful aspects of the factorized spectral surface scenario, while it should not rely on the gauge theory descriptions in 7+1 dimensions. While spectral surfaces can be defined only within the gauge theory descriptions, the essence of the scenario is to keep an unbroken $U(1)$ symmetry in the low-energy effective theory below the Kaluza–Klein scale. We can thus focus on a question whether an unbroken $U(1)$ symmetry is maintained

⁵We will come back to a loophole here in section 4.2.

(or how to find one) in F-theory compactifications. Noting that topological 2-forms of certain type in X_4 yield $U(1)$ vector fields in 3+1 dimensions [20, 21],⁶ and that the vector fields are always accompanied by $U(1)$ symmetries⁷, we see that a solution⁸ is to focus on geometry of X_4 , instead of gauge theory associated with the canonical bundle K_S on S_{GUT} .

Since we are interested in $U(1)$ symmetries under which $SU(5)_{GUT}$ -charged matter fields on S_{GUT} are charged, we are interested in 2-forms of X_4 which have components dual to 2-cycles in the local ALE fiber approximation along S_{GUT} in X_4 . It is a topological problem whether or not an extra $U(1)$ symmetry remains unbroken. We keep tracks of topological 2-forms / 2-cycles to address this problem; it is not necessary to restrict our attention only to 2-cycles contained in one of the A – D – E types, or to 2-cycles that are relatively small. All the 2-cycles in X_4 can be treated in an equal footing, and hence, we are free from all the problems in the gauge theory description on 7+1 dimensions. The factorization condition of the spectral surface for an unbroken $U(1)$ symmetry is replaced by a condition that there is at least one⁹ monodromy-invariant 2-cycle over S_{GUT} .

3 Monodromy of 2-Cycles

In this section, we study monodromy of 2-cycles in a Calabi–Yau 4-fold X_4 and discuss whether an unbroken $U(1)$ symmetry remains or not when the spectral surface satisfies a factorization condition. In section 3.2, we show that certain subgroup of the monodromy corresponds to what we expect from the gauge theory descriptions on 7+1 dimensions. This subgroup reduces to a smaller one when the spectral surface is in the factorization limit, and there is a monodromy invariant 2-cycle [and hence an unbroken $U(1)$] at this level of analysis. This guarantees that we can keep the heart of the idea of the factorized spectral

⁶ These vector fields can be massive, yet global $U(1)$ symmetries may remain in the effective theory. That is the situation we are interested in.

⁷The similar idea that an invariant 2-cycle under the monodromy group gives rise to an unbroken $U(1)$ symmetry, has been applied to the system of D5-branes wrapped on 2-cycles in an ALE fibered geometry [22].

⁸One might alternatively think of factorizing the discriminant as a generalization of factorizing the spectral surface. However, this idea does not work from the very beginning. Global factorization of the *spectral surface* makes sense as a solution to the dimension-4 proton decay problem, because the spectral surface for the $SU(5)_{GUT}$ - $\mathbf{\bar{5}}$ representation is factorized into 2 irreducible branches around points of down-type Yukawa coupling (D_6 singularity enhancement points). As studied in section 4.3 of [4], however, the *discriminant locus* does not have this property. See Figure 10.(b) of [4].

⁹ To be more precise, the condition is the existence of an extra 6-cycle [equivalently its Poincare dual] of X_4 contributing to $H^{1,1}(X)$ other than B_3 or those in $\pi_X^*(H^{1,1}(B_3))$ [20, 21]. We will come back to this issue in section 3.5.

surface scenario without relying on the gauge theory description. Section 3.3 explains the structure of the full monodromy group; the subgroup in section 3.2 is a proper subgroup of the full monodromy group. We study monodromy of 2-cycles for some other generators in section 3.4, and find that there is no monodromy-invariant 2-cycles when the full monodromy group is taken into consideration. This means that there is no unbroken $U(1)$ symmetry in the effective theory in the factorized limit of the spectral surface.

3.1 The model and the notation

In the study of monodromy of 2-cycles in sections 3.2–3.4, we only consider a special case where a Calabi–Yau 4-fold X_4 is a K3 fibration over S_{GUT} : $\pi'_X : X_4 \rightarrow S_{GUT}$. One of the advantages of this X_4 as a global fibration on S_{GUT} is that the $U(1)$ vector fields in 3+1 dimensions, and hence the non- $H^2(B_3)$ non- $H^0(B_3; R^2\pi_{X*}\mathbb{Z})$ components of $H^2(X_4; \mathbb{Z})$ can be studied by $H^0(S_{GUT}; R^2\pi'_{X*}\mathbb{Z})$ [23, 2, 24]. Global sections of the *local* system $R^2\pi'_{X*}\mathbb{Z}$ correspond precisely to the monodromy invariant 2-cycles in the fiber of $\pi'_X : X_4 \rightarrow S_{GUT}$, and hence the problem can be formulated as a local theory on 7+1 dimensions (if not as a local *gauge* theory on 7+1 dimensions). Although this advantage may appear to be available only for a special case, global fibration of X_4 over S_{GUT} , we consider otherwise. Topological 2-cycles in a neighbourhood of S_{GUT} can be captured by a local system like $R^2\pi'_{X*}\mathbb{Z}$ at least locally, if not globally. Since the monodromy among 2-cycles is about a non-trivial local behavior of such a local system at special points (which we call monodromy locus later in this article), one only has to examine local behavior of such local systems to find out whether a $U(1)$ symmetry is projected out or not. Thus, although the following presentation in this section may appear to rely exclusively on a X_4 that is a global fibration on S_{GUT} , we do not lose generality as a study of F-theory compactifications. Discussion on non-K3 fibered cases is found in section 3.5.

The other advantage is that we know a lot about 2-cycles of K3 manifold, so that we can make our presentation very concrete. Since the monodromy around $a_0 = 0$ locus might involve not just 2-cycles within E_8 but also other 2-cycles in the direction transverse to the GUT divisor S_{GUT} , we certainly need a geometry for analysis where such an “other 2-cycle” is identified. With a compact K3 manifold in the transverse direction, we have all the necessary techniques. On the other hand, we do not lose generality by this specific choice, because we are interested only in the local behavior of monodromy among 2-cycles in E_8 and those that are “adjacent” to them.

In principle, we could study monodromy of 2-cycles in a configuration of real interest,

where the A_4 singularity is along S_{GUT} , and a factorization condition is imposed on the 5-fold spectral cover (8). Instead of this realistic $E_8 \rightarrow \text{SU}(5)_{\text{GUT}}$ symmetry breaking model, however, we study monodromy of 2-cycles in an $E_8 \rightarrow E_6$ symmetry breaking model. 2+1 factorization condition can be imposed on the 3-fold spectral cover

$$a_0\xi^3 + a_2\xi + a_3 = 0. \quad (10)$$

Moreover, since the 2-cycles associated with the hidden sector is not essential in our problem, we consider a configuration with an unbroken hidden E_8 symmetry. Namely, we study monodromy of 2-cycles in X_4 whose K3 fibration structure is given by

$$y^2 = x^3 + (a_2z^3 + f_0z^4)x + \left(\frac{1}{4}a_3^2z^4 + a_0z^5 + g_0z^6 + a_0''z^7\right). \quad (11)$$

Here, (x, y) are coordinates of the elliptic fiber of X_4 , z an inhomogeneous coordinate of the base \mathbb{P}^1 of K3 and $a_{0,2,3}, a_0'', f_0, g_0$ are sections of some line bundles on S_{GUT} .

When F-theory is compactified on a K3 manifold that is an elliptic fibration $\pi_{K3} : K3 \rightarrow \mathbb{P}^1$ with a section, then there are 20 2-cycles dual to $H^1(\mathbb{P}^1; R^1\pi_{K3*}\mathbb{Z})$ and corresponding U(1) symmetries in 7+1 dimensions. Such topological 2-cycles can be described by string junctions on the base \mathbb{P}^1 . All the necessary details in how to find independent 20 configuration of such junctions [17] are reviewed in the appendix A.

In order to calculate monodromy of 2-cycles, or equivalently to see how the local system $R^2\pi'_{X*}\mathbb{Z}$ is twisted, one first has to take a base point $b \in S_{GUT}$, and set a basis in the (co)homology group of $H_2(\pi'^{-1}_X(b); \mathbb{Z}) \simeq H_2(K3; \mathbb{Z})$. For a loop γ on S_{GUT} that starts and ends on the base point b , we can trace the basis elements $H_2(\pi'^{-1}_X(p); \mathbb{Z})$ for points p on the loop γ , starting from the base point b until we come back to the base point again. The calculation of monodromy is practically carried out by tracing string junction configuration that correspond to the basis elements of $H_2(\pi'^{-1}_X(b); \mathbb{Z})$. We only have to trace along the loop γ the motion of discriminant locus points— $[p, q]$ 7-branes—in the complex z plane. All the necessary techniques in this monodromy analysis is quite standard in Type IIB string theory. We thus present detailed procedure of practical calculation of monodromy for only three loops in the appendix A; for all other loops, only the results are presented in this article.

It is convenient to introduce a notation for a set of independent 2-cycles of the K3 fiber and also to assign names to individual $[p, q]$ 7-branes at a base point b . To the 24 discriminant points, we assign the following names: $A8$ – $A1$, B , $C1$, $C2$, D , $A8'$ – $A1'$, B' , $C1'$, $C2'$ and D' . The appendix A explains the choice of the base point b , location of the the 24 7-branes in the

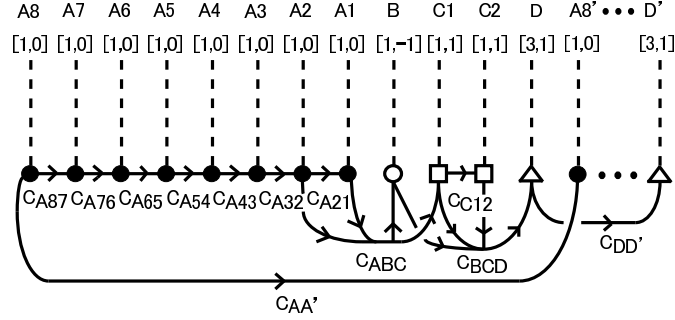


Figure 1: The independent 2-cycles of a K3 surface. Dotted lines represent the branch cuts of 7-branes. Black blobs represent A -branes, open circles are B -branes, open boxes correspond to C -branes and open triangles are “ D ”-branes whose $[p, q]$ charge is $[3, 1]$. $A8' \sim D'$ 7-branes have the same $[p, q]$ charges as those without a $'$, and are ordered from left to right as in the same way as $A8 \sim D$ 7-branes. 7-branes from $A7$ to $C2$ and those from $A7'$ to $C2'$ constitute separate sets of $[A^7 BC^2]$ 7-brane configuration of E_8 .

2-cycles inside E_8	$C_{A76}, C_{A65}, C_{A54}, C_{A43}, C_{A32}, C_{A21}, C_{ABC}, C_{C12}$
2-cycles outside E_8	$C_\alpha^1, C_\alpha^2, C_\beta^1, C_\beta^2$
those for hidden E_8	$C'_{A76}, C'_{A65}, C'_{A54}, C'_{A43}, C'_{A32}, C'_{A21}, C'_{ABC}, C'_{C12}$

Table 1: A convenient choice of a basis of $H_2(\pi'^{-1}(b); \mathbb{Z})$.

z plane, as well as their $[p, q]$ charges for the base point. We assign names (notation) such as C_{A76} , C_{A65} etc. to string junction configurations and corresponding 2-cycles of $K3 = \pi'^{-1}(b)$. All the details are written in the appendix A, but the most relevant part of the information is summarized in Figure 1.

There is no unique choice of a basis of $H_2(K3; \mathbb{Z})$, but one of the most convenient choices is to use the 2-cycles listed in Table 1. Among them, $C_\alpha^{1,2}$, C_β^2 need to be defined by linear combinations of string junction configurations like those in Figure 1; see (75, 76). The intersection form becomes (74). The intersection form within the eight 2-cycles in the first row of Table 1 is described by the Dynkin diagram of E_8 shown in Figure 2.

As we study monodromy of 2-cycles in (11) that has unbroken E_6 symmetry (split form E_6 singularity) [18], monodromy matrices must be trivial on a subspace generated purely by $C_{A54}, C_{A43}, C_{A32}, C_{A21}, C_{ABC}, C_{C12}$, the simple roots of E_6 . Thus, we can choose $C_{-\theta}$ as a basis element instead of C_{A65} as in Table 1, where $C_{-\theta}$ is a linear combination purely of the

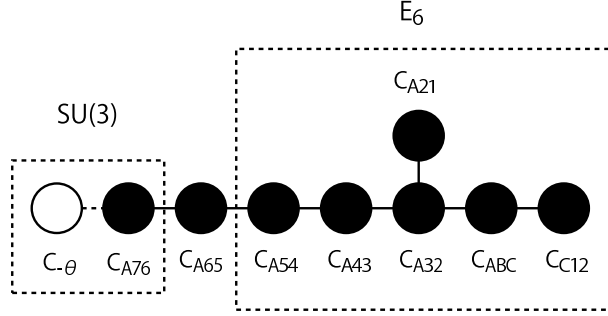


Figure 2: 2-cycles inside E_8 and their intersection. Note that $C_{-\theta}$ is not the same as C_{A87} ; see footnote 24 for more.

2-cycles in the first row of Table 1,

$$C_{-\theta} = -(2C_{A76} + 3C_{A65} + 4C_{A54} + 5C_{A43} + 6C_{A32} + 4C_{ABC} + 3C_{A21} + 2C_{C12}). \quad (12)$$

The six 2-cycles of E_6 and the two 2-cycles C_{A76} and $C_{-\theta}$ for the “structure group” $SU(3)_{\text{str}}$ are orthogonal in the intersection form. Since we restrict ourselves in a region of moduli space where the hidden E_8 2-cycles do not participate in the monodromy, the monodromy can be represented by 6×6 matrices acting on a vector space generated by $C_{A76}, C_{-\theta}, C_{\alpha}^1, C_{\alpha}^2, C_{\beta}^1$ and C_{β}^2 .

The calculation of monodromy boils down to following the trace of the $[p, q]$ 7-branes along paths in S_{GUT} . Thus, an explicit expressions for the discriminant of (11) is very useful:

$$\Delta = z^8 \Delta' \quad (13)$$

where Δ' is given by

$$\begin{aligned} \Delta' = & \frac{27}{16}a_3^4 + \left(\frac{27}{2}a_0a_3^2 + 4a_2^3 \right) z + \left(\frac{27}{2}a_3^2g_0 + 27a_0^2 + 12a_2^2f_0 \right) z^2 \\ & + \left(54a_0g_0 + 12a_2f_0^2 + \frac{27}{2}a_3^2a_0'' \right) z^3 + (4f_0^3 + 27g_0^2 + 54a_0a_0'')z^4 \\ & + 54a_0''g_0z^5 + 27a_0''^2z^6. \end{aligned} \quad (14)$$

In this model, eight 7-branes $A5$ – $A1$ and $B, C1, C2$ are at an E_6 singularity at $z = 0$ [25, 26], and ten 7-branes $A7'$ – $A1', B', C1'$ and $C2'$ form an E_8 singularity at $z = \infty$. The six other 7-branes, $A6, A7, A8, D, A8'$ and D' , are the zero points of Δ' above. Along a path γ in S_{GUT} , values of all the coefficients $a_{0,2,3}, f_0, g_0$ and a_0'' change, and hence the six 7-branes

change their locations in the z -plane. We can thus determine the monodromy matrix by following the 7-branes and string junctions.

In sections 3.2–3.4, we present monodromy matrices obtained as a result of such a calculation. Although the monodromy for a loop γ in S_{GUT} is ultimately what we are interested in, it is a better idea to study monodromy of 2-cycles in a little more abstract level; we will study monodromy of 2-cycles for loops in a moduli space of an elliptic K3 manifold. Since any loops in S_{GUT} are mapped by the choice of sections $a_{0,2,3}$, f_0 etc. to loops in the moduli space of the elliptic K3 manifold, the monodromy group for the loops on S_{GUT} is obtained by a pull-back of the monodromy group for the loops on the elliptic K3 moduli space by the sections. Such questions as whether an unbroken $U(1)$ symmetry exists can be answered at the level of monodromy on the elliptic K3 moduli space, independent of specific details of S_{GUT} or sections $a_{0,2,3}$ etc. on it.

3.2 The monodromy in 8D gauge theory region

In the factorization limit of the spectral surface, the monodromy group of 2-cycles captured in the gauge theory description on 7+1 dimensions is reduced; there is no question about this statement in the deformation of A_{N+M} singularity to A_M . This statement is believed to be true also in deformation of $E_{6,7,8}$ type singularity to A_4 [4, 6] (see also [2]), for example, but it has not been confirmed directly so far by looking at 2-cycles in X_4 . In this section 3.2, we study explicitly the geometry of 2-cycles in X_4 when the spectral surface is at the factorization limit, and confirm that the statement above is correct. This justifies our strategy to replace the factorization limit of spectral surfaces by existence of monodromy invariant 2-cycles.

At the same time, we will see that the monodromy of 2-cycles that appear in the gauge theory description on 7+1 dimensions is only a proper subgroup of the entire monodromy group of the whole theory. Thus, it will be clear what one overlooks in the gauge theory description on 7+1 dimensions.

The family of elliptic K3 manifold (11) is parametrized by $(a_0, a_2, a_3, f_0, g_0, a_0'')$, among which two are redundant because of the freedom to rescale the coordinates (x, y, z) . Instead of using a set of “gauge invariant” parameters of this moduli space such as $(a_0 a_0''/g_0^2)$ and $(a_2/a_0)(4f_0^3 + 27g_0^2)^{1/6}$, we fix a gauge by fixing the values of f_0 (or g_0) and a_0'' .

The full scope of the problem is to consider all possible loops in the moduli space of (11) and determine the monodromy of 2-cycles of the K3 for the loops. We restrict our attention

in this section, however, to a subset of the moduli space

$$a_0 = a_{0,*}\epsilon_\eta, \quad a_2 = a_{2,*}\epsilon_K^2\epsilon_\eta, \quad a_3 = a_{3,*}\epsilon_K^3\epsilon_\eta, \quad (15)$$

where parameters $a_{r,*} \in \mathbb{C}$ and $g_0 \in \mathbb{C}$ are at most $\mathcal{O}(1)$; $0 \neq |\epsilon_K| \ll 1$ and $0 \neq |\epsilon_\eta| \ll 1$ are fixed numbers, and we fix the “gauge” by setting $f_0 = -1$ and $a_0'' = \epsilon_\eta$. Because $|\epsilon_\eta| \ll 1$, the elliptic K3 manifold is always close to the stable degeneration limit [20, 27] within the subset specified above. We call this subset scaling region. It helps in ensuring the validity of the gauge theory description in 7+1 dimensions, but not quite, to set ϵ_K as a small number. We will see this in detail in the rest of this section in F-theory language. The appendix B will provide a very clear explanation of this in the dual Heterotic language. The base point of the moduli space is chosen within this subset, and only loops that stay within this subset are considered in this section. Although this is only to find part of the monodromy group, we will see that this partial result is interesting enough from mathematical and physical points of view, and is also sufficient in drawing conclusions for practical purposes.

We will call a subset of the scaling region characterized by

$$|\epsilon_K|^2 \ll |a_{0,*}| \sim \mathcal{O}(1) \quad (16)$$

as an *8D gauge theory region*. We will see in this section 3.2 that all the loops (except the one mentioned at the end of section 3.4) that stay within this “8D gauge theory region” yield monodromies of 2-cycles that are expected from the gauge theory descriptions on 7+1 dimensions.

For any points in the 8D gauge theory region of the moduli space, the six 7-branes specified by $\Delta' = 0$ are distributed in the complex z plane as follows; there are two 7-branes in the region $z \sim \mathcal{O}(\epsilon_K^6\epsilon_\eta)$, two in the region $z \sim \mathcal{O}(\epsilon_\eta)$, and two in $z \sim \mathcal{O}(\epsilon_\eta^{-1})$. These three groups of 7-branes remain distinct along any loops that stay within the 8D gauge theory region of the moduli space. It is, thus, appropriate to identify that the two 7-branes in the $\mathcal{O}(\epsilon_\eta^{-1})$ region as the 7-branes $A8'$ and D' , those in the $\mathcal{O}(\epsilon_\eta)$ region as $A8$ and D , and those in the $\mathcal{O}(\epsilon_K^6\epsilon_\eta)$ region as $A6$ and $A7$, respectively. Over the entire 8D gauge theory region, the positions of the 7-branes $A6$, $A7$ are effectively given by the zero points of

$$\Delta'_{\text{lower-quadr}} = \frac{27}{16}a_3^4 + \left(\frac{27}{2}a_0a_3^2 + 4a_2^3\right)z + 27a_0^2z^2, \quad (17)$$

which is approximately the first three terms of the right hand side of (14).

The string junction configuration (and the corresponding 2-cycles) C_{A76} and $C_{-\theta}$ correspond to the two roots of $\text{SU}(3)_{\text{str}}$, the commutant of E_6 within E_8 . As a point moves along a

loop in (the 8D gauge theory region of) the moduli space, the coefficients $a_{0,2,3}$ in (17) change, and the positions of the $A7$ and $A6$ 7-branes move in the complex z -plane. Consequently the branch cuts and the string junction configurations also have to change continuously. Monodromy of the two 2-cycles C_{A76} and $C_{-\theta}$ should reproduce what we expect from the 8D gauge theory descriptions.

Such loops in the moduli space should avoid a locus where more than one 7-branes come on top of one another, because the elliptic K3 “manifold” becomes singular and it is subtle to talk of “topological 2-cycles” there. The degeneration of the $A6$ and $A7$ 7-brane positions are characterized by the discriminant locus of the quadratic equation $\Delta'_{\text{lower-quadr}} = 0$:

$$\tilde{\Delta}_{\text{lower-quadr}} = 4a_2^3(27a_0a_3^2 + 4a_2^3) = 0. \quad (18)$$

As one moves on a loop around such a locus of degeneration of the 7-brane positions, $\tilde{\Delta} = 0$, more than one 7-branes may exchange their positions at the end of the loop. Moreover, branch cuts may have to be rearranged in case of degeneration of mutually non-local $[p, q]$ 7-branes. Thus, the locus of 7-brane degeneration is where monodromy of 2-cycles could be generated, and hence we call $\tilde{\Delta} = 0$ locus as the monodromy locus.

The monodromy locus in the 8D gauge theory region is given by (18) [see also section 3.3]. Interestingly the second factor of (18) is the same as the ramification locus of the spectral surface (10). Since we expect a monodromy among 2-cycles along the ramification locus of the spectral surface in the gauge theory description on 7+1 dimensions, it is more than natural that the same factor appears in the monodromy locus that we introduced in the language of X_4 . The first factor of the monodromy locus, $a_2 = 0$ with a multiplicity 3, on the other hand, does not appear in the gauge theory description. We thus move on to calculate the monodromy matrices explicitly to clarify the relation between the two descriptions.

3.2.1 Monodromy without factorization

We begin with a general choice of complex structure without a factorization of (10) in section 3.2.1. From the gauge theory description on 7+1 dimensions, we expect that the monodromy of the 2-cycles C_{A76} and $C_{-\theta}$ is the full Weyl group of $SU(3)_{\text{str}}$, S_3 , and there is no mixing between the 2-cycles in the visible E_8 and others in $H_2(K3; \mathbb{Z})$. Moreover, we expect that the monodromy is generated along the ramification locus $(27a_0a_3^2 + 4a_2^3) = 0$, but nowhere else. These expectations are indeed confirmed by explicit calculations of the monodromy, as we explain in the following.

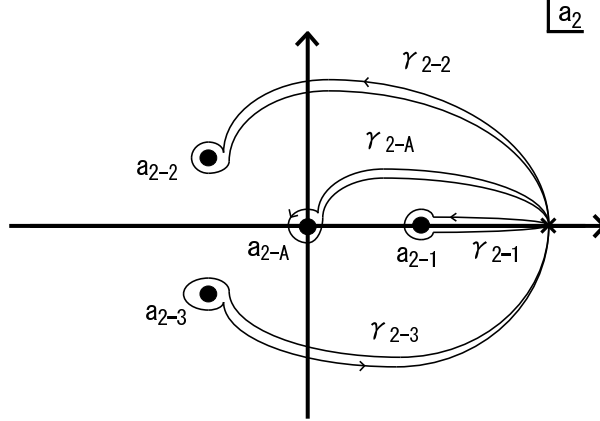


Figure 3: The monodromy locus $\tilde{\Delta}_{\text{lower-quadr}} = 0$ in (18) on the a_2 -plane and independent loops around these points. $a_2 = a_{2-A}$ is a triple point and correspond to the first factor $a_2 = 0$ of $\tilde{\Delta}_{\text{lower-quadr}}$. $a_2 = a_{2-1,2,3}$ are single points, correspond to the second factor of $\tilde{\Delta}_{\text{lower-quadr}}$. The base point is denoted by a cross mark.

Let us pick a base point in the moduli space, and fix it once and for all. All the loops start and end at the base point. We choose it in the 8D gauge theory region:

$$(a_0, a_2, a_3) = (a_{0,0}, a_{2,0}, a_{3,0}) \equiv (1, \epsilon_K^2, i\delta\epsilon_K^3)\epsilon_\eta, \quad (19)$$

with real positive small numbers ϵ_K and ϵ_η . δ is also a small real positive number, which does not play an important role in this article. We set $g_0 = g_{0,0} \equiv 1$ at the base point. Arrangement of the branch cuts and the $[p, q]$ charges of the 7-branes are described explicitly in the appendix A for this choice of the base point.

Although we could study monodromy of all the loops in the 8D gauge theory region of the moduli space parametrized by (a_0, a_2, a_3, g_0) , it just introduces a mess that is not essential to the problem. Instead, let us take a slice of constant $a_0 = a_{0,0}$, $a_3 = a_{3,0}$ and $g_0 = g_{0,0}$ of the moduli space, and consider loops in the complex a_2 -plane.

On the a_2 -plane, the monodromy locus $\tilde{\Delta}_{\text{lower-quadr}} = 0$ consists of one point a_{2-A} with a multiplicity 3, and three points a_{2-1} , a_{2-2} and a_{2-3} with multiplicity 1. Figure 3 shows four independent non-trivial loops in the a_2 -plane. We calculate the monodromy for these four loops. The calculation itself is straightforward, and we just quote the results in this article; calculations for γ_{2-A} and γ_{2-2} here and γ_{0-4} that appears later, however, are explained explicitly in the appendix A in detail as samples.

It turns out that the monodromy associated with γ_{2-A} is trivial. This is consistent with

the expectation that the monodromy is generated only at the second factor of the monodromy locus (18), not at the $a_2 = 0$ factor.

Next we consider the loops γ_{2-1} , γ_{2-2} and γ_{2-3} . The monodromy associated with γ_{2-2} is explicitly computed in the appendix A to give the result

$$\begin{aligned}\tilde{C}_{A65} &= C_{-\theta} + C_{A65} + C_{A76}, \\ \tilde{C}_{A76} &= -C_{-\theta}, \\ \tilde{C}_{-\theta} &= -C_{A76},\end{aligned}\tag{20}$$

while $C_\alpha^{1,2}$ and $C_\beta^{1,2}$ are left invariant. Here \tilde{C}_i denotes the transformed 2-cycle of C_i after going along γ_{2-2} . Similarly, the monodromies associated with γ_{2-1} and γ_{2-3} can be computed. The result for γ_{2-1} is

$$\begin{aligned}\tilde{C}_{A65} &= C_{A76} + C_{A65}, \\ \tilde{C}_{A76} &= -C_{A76}, \\ \tilde{C}_{-\theta} &= C_{A76} + C_{-\theta}\end{aligned}\tag{21}$$

and, for γ_{2-3} , the same monodromy as (20) is obtained. Thus, the monodromy for these three loops act only on the 2-dimensional subspace of $H_2(\text{K3}; \mathbb{Z})$ generated by C_{A76} and $C_{-\theta}$, and are trivial on all the six generators of the visible E_6 , all the eight generators of the hidden E_8 and all the four 2-cycles $C_{\alpha,\beta}^{1,2}$ in the middle. These monodromies were generated essentially around the $(27a_0a_3^2 + 4a_2^3) = 0$ locus. This is also consistent with the expectation.

It is not difficult to see that these monodromy transformation on the visible E_8 2-cycles are regarded as Weyl reflections of $\text{SU}(3)_{\text{str}} \subset E_8$. The monodromy $\rho(\gamma_{2-1})$ is a Weyl reflection generated by a root C_{A76} , $W_{C_{A76}}$, and $\rho(\gamma_{2-2})$ and $\rho(\gamma_{2-3})$ are $W_{C_{A76}+C_{-\theta}}$. When they are represented on a three-element basis, $(C_{A65}, C_{A65} + C_{A76}, C_{A65} + C_{A76} + C_{-\theta})$, they become

$$\rho_{\mathbf{3}}(\gamma_{2-1}) = \begin{pmatrix} 0 & 1 & 0 \\ 1 & 0 & 0 \\ 0 & 0 & 1 \end{pmatrix}\tag{22}$$

$$\rho_{\mathbf{3}}(\gamma_{2-2}) = \rho_{\mathbf{3}}(\gamma_{2-3}) = \begin{pmatrix} 0 & 0 & 1 \\ 0 & 1 & 0 \\ 1 & 0 & 0 \end{pmatrix}.\tag{23}$$

Thus, they generate the permutation group S_3 , the full Weyl group of $\text{SU}(3)_{\text{str}}$, just as expected in the gauge theory description without a factorization of the spectral surface.

3.2.2 Monodromy with factorization

It is known that in the gauge theory description on 7+1 dimensions, if we impose a factorization condition on a spectral surface, then the structure group is reduced and an unbroken $U(1)$ symmetry appears. In the remainder of this subsection, we will see that this fact can be described in terms of the monodromies of 2-cycles as well.

On the spectral surface (10), let us impose the 2+1 factorization condition [10, 11]

$$0 = a_0 \xi^3 + a_2 \xi + a_3 = (c_0 \xi^2 + c_1 \xi + c_2)(d_0 \xi + d_1) \quad (24)$$

for some sections $c_{0,1,2}$ and $d_{0,1}$ on S_{GUT} . These sections have to satisfy a condition [11]

$$c_0 d_1 + c_1 d_0 = 0, \quad (25)$$

and we adopt a solution to this condition, $d_0 = c_0$ and $d_1 = -c_1$. Thus,

$$a_0 = c_0^2, \quad (26)$$

$$a_2 = c_0 c_2 - c_1^2, \quad (27)$$

$$a_3 = -c_1 c_2. \quad (28)$$

We now consider a family of elliptic K3 manifold parametrized by (c_0, c_1, c_2, g_0) , and study monodromy of 2-cycles for loops in this moduli space.

The 8D gauge theory region in the (c_0, c_1, c_2, g_0) space is characterized by

$$c_0 = c_{0,*} \epsilon_\eta^{1/2}, \quad c_1 = c_{1,*} \epsilon_K \epsilon_\eta^{1/2}, \quad c_2 = c_{2,*} \epsilon_K^2 \epsilon_\eta^{1/2}, \quad (29)$$

where parameters $c_{r,*} \in \mathbb{C}$ ($r = 0, 1, 2$) and $g_0 \in \mathbb{C}$ are at most $\mathcal{O}(1)$. ϵ_K and ϵ_η are small but non-zero parameters as before. We further require that

$$\epsilon_K \ll |c_{0,*}| \sim \mathcal{O}(1). \quad (30)$$

We will take a base point as

$$(c_0, c_1, c_2) = (c_{0,0}, c_{1,0}, c_{2,0}) \equiv (1, -i\epsilon_K, \delta' \epsilon_K^2) \epsilon_\eta^{1/2}, \quad (31)$$

and $g_0 = g_{0,0} = 1$; real positive values are used for small numbers ϵ_K , ϵ_η and δ' , so that this base point is mapped to the base point in the (a_0, a_2, a_3, g_0) parameter space through (26–28).

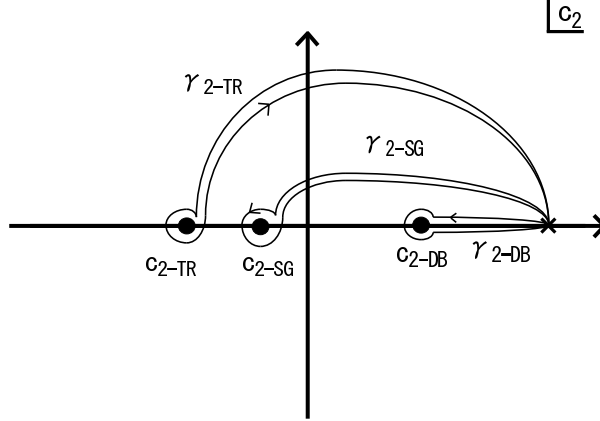


Figure 4: The monodromy locus $\tilde{\Delta}_{\text{lower-quad}} = 0$ on the c_2 -plane and independent loops around these points. The cross mark is the base point $c_2 = c_{2,0}$.

The monodromy locus in the 8D gauge theory region in the (c_0, c_1, c_2, g_0) parameter space is given by simply rewriting (18) by (26–28). It factorizes as

$$\tilde{\Delta}_{\text{lower-quad}} = 4(c_0 c_2 - c_1^2)^3 (4c_0 c_2 - c_1^2) (c_0 c_2 + 2c_1^2)^2. \quad (32)$$

If we focus on a constant c_0, c_1, g_0 slice (complex c_2 -plane) of the moduli space that contains the base point, then the monodromy locus $\tilde{\Delta}_{\text{lower-quad}} = 0$ consists of three points; see Figure 4. One of them c_{2-TR} is a triple point, another c_{2-SG} a single point, and the other c_{2-DB} a double point; they correspond to the zero locus of the first, second and the last factor of (32), respectively. Three independent non-trivial loops are contained in this slice (Figure 4), and we study the monodromy of 2-cycles for these loops.

Since the loops $\gamma_{2-TR}, \gamma_{2-SG}$ and γ_{2-DB} are mapped, respectively, to $\gamma_{2-A}, \gamma_{2-3}$ and $(\gamma_{2-1})^2$ by (26–28) topologically, the monodromies are given by $\rho(\gamma_{2-TR}) = \rho(\gamma_{2-A}) = \text{id.}$, $\rho(\gamma_{2-SG}) = \rho(\gamma_{2-3})$ and $\rho(\gamma_{2-DB}) = (\rho(\gamma_{2-1}))^2 = \text{id.}$ Therefore, the full monodromy group of the 2-cycles for these loops is generated only by

$$\rho(\gamma_{2-SG}) = W_{C_{A76} + C_{-\theta}} \simeq \mathbb{Z}_2. \quad (33)$$

The monodromy group is reduced from the full Weyl group S_3 of $\text{SU}(3)_{\text{str}}$ to its \mathbb{Z}_2 subgroup, and the 2-cycle C_{A76} is monodromy invariant.

The reduction of the monodromy group is a direct consequence of the factorization limit (24); the $(27a_0 a_3^2 + 4a_2^3) = 0$ component of the monodromy locus factorized as in (32), and one

of the irreducible pieces become multiplicity two. That is essential in making the monodromy $\rho(\gamma_{c_2-DB})$ trivial. The remaining monodromy is generated essentially around $(c_1^2 - 4c_0c_2) = 0$, which is precisely the ramification locus of the 2-fold spectral cover in the 2+1 factorization limit. All these results obtained in terms of monodromy of 2-cycles in elliptic K3 manifold agree with the expectation from the gauge theory description on 7+1 dimensions.

3.3 The “Full” Monodromy Group

In the previous subsection, we focused on the a_2 -plane in the 8D gauge theory region and reproduced the expected monodromy group by looking directly at the monodromy of 2-cycles. Thus, we can use the monodromy of the 2-cycles to study physics/geometry that cannot be described precisely in the gauge theory description on 7+1 dimensions.

As discussed in section 2, the gauge theory description on 7+1 dimensions have two independent difficulties. The problem A was that one has no choice but to drop terms that either are higher order in the z' coordinate expansion, or have coefficients suppressed by ϵ_K , in order to fit the geometry into an E_8 gauge theory. This approximation corresponds to using (17) instead of (14) by dropping higher order terms. Thus, this problem of the gauge theory description can be overcome by simply repeating the same monodromy analysis for (14) by keeping higher order terms.

The other difficulty of the gauge theory description, the problem B, was how to formulate a region near the $a_0 = 0$ locus in S_{GUT} . In order to study the geometry of an elliptic K3 manifold near the $a_0 = 0$ region of the moduli space, we only have to follow loops that step into the $a_0 \simeq 0$ region and calculate the monodromy, just like we did for loops that stay within the 8D gauge theory region.

In order to study the full monodromy in the scaling region (15) without staying strictly in the 8D gauge theory region (16), it is no longer possible to maintain only the lower quadratic terms from (14). As $|a_{0,*}|$ becomes much smaller than 1 and comes closer to $|\epsilon_K^2|$, one of the two 7-branes in the $z \sim \mathcal{O}(\epsilon_K^6 \epsilon_\eta)$ region behaves as

$$z_i \simeq -\frac{4}{27} \frac{a_2^3}{a_0^2} \sim \mathcal{O}(\epsilon_\eta \epsilon_K^6) \times \frac{1}{a_{0,*}^2}. \quad (34)$$

This behavior in terms of the discriminant locus corresponds to (9) in terms of the spectral surface. At the same time, the two 7-branes in the $z \sim \mathcal{O}(\epsilon_\eta)$ region move as $z_i \sim a_0 = \epsilon_\eta a_{0,*}$. Thus, the three 7-branes come close to one another when $a_{0,*}$ is as small as ϵ_K^2 . Those 7-branes are no longer clearly separated into the groups of [A6 + A7] and [A8 + D]. We should

use at least quartic polynomial part of (14).

Monodromy of 2-cycles are (potentially) generated only around a locus in the moduli space where more than one 7-branes come on top of the other(s). Thus, the monodromy locus on the moduli space is characterized by the discriminant locus $\tilde{\Delta} = 0$ of a polynomial $\Delta'(z) = 0$ in (14) that determines the positions of the 7-branes. $\tilde{\Delta} = 0$ defines a divisor in the moduli space. Monodromy of 2-cycles should be calculated for loops on the moduli space that stay away from the monodromy locus. Therefore, the full monodromy group is a representation of the fundamental group of the moduli space without the monodromy divisor. There is no essential difficulty in approaching the $a_0 \simeq 0$ region, or incorporating higher order terms of the $\Delta'(z)$ polynomial.

As long as we stay within the scaling region (15) with an $a_0'' = \epsilon_\eta \neq 0$ gauge, however, the problem becomes a little easier. The two 7-branes $[A8' + D']$ stay within the $z \sim \mathcal{O}(\epsilon_\eta^{-1})$ region, and are frozen out there; we thus only need to follow the behavior of the four other 7-branes. We can now use

$$\begin{aligned} \Delta'_\eta = & \frac{27}{16}a_3^4 + \left(\frac{27}{2}a_0a_3^2 + 4a_2^3\right)z + \left(\frac{27}{2}a_3^2g_0 + 27a_0^2 + 12a_2^2f_0\right)z^2 \\ & + (54a_0g_0 + 12a_2f_0^2)z^3 + (4f_0^3 + 27g_0^2)z^4 \end{aligned} \quad (35)$$

instead of (14) or (17).

The monodromy divisor in the moduli space is the discriminant locus of $\Delta'_\eta(z) = 0$:

$$\tilde{\Delta}_\eta = -19683A^3B = 0, \quad (36)$$

where A and B are given by

$$A = 4a_0a_2f_0 - a_3^2f_0^2 - 4a_2^2g_0, \quad (37)$$

$$\begin{aligned} B = & 4a_0^3a_2^3 + 27a_0^4a_3^2 + 4a_0a_2^5f_0 + 30a_0^2a_2^2a_3^2f_0 - a_2^4a_3^2f_0^2 - 24a_0a_2a_3^4f_0^2 \\ & + 4a_3^6f_0^3 - 4a_2^6g_0 - 36a_0a_2^3a_3^2g_0 - 54a_0^2a_3^4g_0 + 18a_2^2a_3^4f_0g_0 + 27a_3^6g_0^2. \end{aligned} \quad (38)$$

$\tilde{\Delta}_{\text{lower-quadr}}$ in (18) is reproduced¹⁰ by keeping only the leading order terms in ϵ_K in (37) and (38):

$$A_{\text{leading}} = 4a_0a_2f_0, \quad (39)$$

$$B_{\text{leading}} = a_0^3(4a_2^3 + 27a_0a_3^2). \quad (40)$$

¹⁰ The triple point a_{2-A} and the three points $a_{2-1,2,3}$ on the a_2 -plane are obtained as the roots of $A = 0$ and $B = 0$; all of a_0 , a_3 and g_0 are treated as fixed numbers here. Although B is an order-six polynomial of a_2 , the remaining three roots are not in the scaling region $a_{2,*} \lesssim \mathcal{O}(1)$.

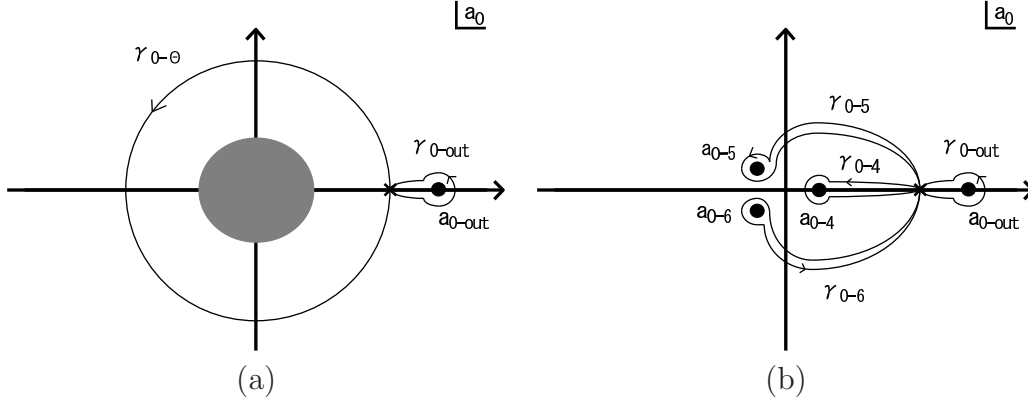


Figure 5: The $B = 0$ component of the monodromy locus consists of four points on the a_0 -plane containing the base point (cross mark). Among them, only a_{0-out} lies in the 8D gauge theory region $|\epsilon_K^2 \epsilon_\eta| \ll |a_0|$, and all others $a_{0-4,5,6} \sim \mathcal{O}(\epsilon_K^2 \epsilon_\eta)$ are located outside of the 8D gauge theory region (in a shaded region in (a)).

In order to see study the monodromy associated with the $a_0 \simeq 0$ region, it is useful to take a slice of the moduli space at constant a_2 , a_3 and g_0 with a free a_0 , and look at the distribution of the monodromy divisor in the complex a_0 plane. We take a slice that contains the base point (19). The $B = 0$ component of the monodromy locus appears in the a_0 plane as in Figure 5. There is only one monodromy locus a_{0-out} in the 8D gauge theory region $|\epsilon_K^2 \epsilon_\eta| \ll |a_0|$, but three new types of monodromy loci appear in the $a_0 \sim \mathcal{O}(\epsilon_K^2 \epsilon_\eta)$ region. We can think of various loops drawn in Figure 5; it is clearly a question of interest what the monodromy of 2-cycles will be for those loops.

Note that we do not have to consider the $A = 0$ component of the monodromy locus any more. In section 3.2, we see that the monodromy of the loop γ_{2-A} is trivial. For any loops γ_A in the moduli space (except $A = 0$ and $B = 0$) that are homotopic to a loop of the form

$$\gamma_A = \gamma_B^{-1} \circ \gamma_{2-A} \circ \gamma_B \quad (41)$$

for some loop γ_B , $\rho(\gamma_A) = \text{id.}$, because $\rho(\gamma_{2-A}) = \text{id.}$. Thus, we focus only on the monodromy of the loops which go around the $B = 0$ component (38) in the following.

Among the loops in the a_0 plane in Figure 5, γ_{0-out} and $\gamma_{0-\theta}$ stay within the 8D gauge theory region of the moduli space. Direct computation of the monodromy $\rho(\gamma_{0-out})$ shows that

$$\rho(\gamma_{0-out}) = W_{C_{A76}} = \rho(\gamma_{2-1}). \quad (42)$$

This is actually expected, because the loop γ_{0-out} is homotopic to γ_{2-1} in the (a_0, a_2, a_3, g_0) moduli space without the $B = 0$ monodromy locus. One can also see that $\gamma_{2-2} \sim \gamma_{0-\theta} \circ \gamma_{0-out} \circ \gamma_{0-\theta}^{-1}$ and $\gamma_{2-3} \sim \gamma_{0-\theta}^{-1} \circ \gamma_{0-out} \circ \gamma_{0-\theta}$, and hence the following relations

$$\rho(\gamma_{0-\theta})\rho(\gamma_{0-out})\rho(\gamma_{0-\theta})^{-1} = \rho(\gamma_{2-2}) = W_{C_{A76}+C_{-\theta}}, \quad (43)$$

$$\rho(\gamma_{0-\theta})^{-1}\rho(\gamma_{0-out})\rho(\gamma_{0-\theta}) = \rho(\gamma_{2-3}) = W_{C_{A76}+C_{-\theta}} \quad (44)$$

should hold true. We confirmed these relations by explicit computation of the monodromy¹¹ $\rho(\gamma_{0-\theta})$. Other loops in Figure 5 in the a_0 plane, which go away from the 8D gauge theory region of the moduli space, are not homotopic at least apparently to the loops whose monodromy we have already calculated.

The full monodromy group of the 2-cycles is a representation of the fundamental group of the (a_0, a_2, a_3, g_0) moduli space from which the $B = 0$ monodromy locus is deleted, and this is what we are interested in. The monodromy group observed in the gauge theory description on 7+1 dimensions, however, correspond to the representation of a subgroup generated only by loops that stay within the 8D gauge theory region of the moduli space. The monodromy group on the 2-cycles split into direct product of the one on $\text{Span}_{\mathbb{Z}}\{C_{A76}, C_{-\theta}\}$ and the one on $\text{Span}_{\mathbb{Z}}\{C_{\alpha,\beta}^{1,2}\}$ at this level of analysis. The loops such as $\gamma_{0-4,5,6}$ in Figure 5, however, may not be contained in this subgroup, and in general, the full monodromy group is larger than the expectation from the gauge theory description on 7+1 dimensions. Exactly the same thing can be said about the monodromy group of 2-cycles of a family of elliptic K3 manifold parametrized by (c_0, c_1, c_2, g_0) .

3.4 The monodromy beyond the 8D gauge theory region

We first show that the full monodromy group of the family (11) with (a_0, a_2, a_3, g_0) moduli space is indeed larger than the monodromy group expected from the gauge theory description on 7+1 dimensions. This is done by calculating the monodromy of the loops $\gamma_{0-4,5,6}$ in Figure 5; this is to probe physics and geometry of a region of small a_0 , where the E_8 gauge theory description on 7+1 dimensions breaks down. We then move on to study the monodromy group of the family for the factorization limit parametrized by (c_0, c_1, c_2, g_0) .

The monodromy for the loops $\gamma_{0,4,5,6}$ can be computed by the same method as in the preceding sections; the calculation for the loop γ_{0-4} is demonstrated explicitly in the appendix

¹¹ The monodromy matrix $\rho(\gamma_{0-\theta})$ splits into a 2 by 2 block on $\text{Span}_{\mathbb{Z}}\{C_{A76}, C_{-\theta}\}$ and a 4 by 4 block $\text{Span}_{\mathbb{Z}}\{C_{\alpha,\beta}^{1,2}\}$. It is a Weyl reflection $W_{C_{-\theta}}$ in the former. In the latter, $\tilde{C}_{\alpha,\beta}^1 = C_{\alpha,\beta}^1$, $\tilde{C}_{\alpha}^2 = C_{\alpha}^2 - C_{\beta}^1$ and $\tilde{C}_{\beta}^2 = C_{\beta}^2 + C_{\alpha}^1$. The monodromy still splits between the visible E_8 sector and others for this loop $\gamma_{0-\theta}$.

A. It turns out that the monodromy of γ_{0-4} is

$$\begin{aligned}\tilde{C}_{A65} &= C_{A65}, & \tilde{C}_{A76} &= C_{A76} + C_{-\theta} - C_{\alpha}^1, \\ \tilde{C}_{\alpha}^1 &= C_{\alpha}^1, & \tilde{C}_{\alpha}^2 &= C_{\alpha}^2 + C_{\alpha}^1 - C_{-\theta}, \\ \tilde{C}_{\beta}^1 &= C_{\beta}^1, & \tilde{C}_{\beta}^2 &= C_{\beta}^2,\end{aligned}\tag{45}$$

or equivalently,

$$\rho(\gamma_{0-4}) = \left(\begin{array}{cc|cc|c} 1 & & & & \\ 1 & -1 & & -1 & \\ \hline -1 & 2 & 1 & 1 & \\ & & & 1 & \\ \hline & & & & \mathbf{1}_{2 \times 2} \end{array} \right)\tag{46}$$

when we choose the basis as $(C_{A76}, C_{-\theta}, C_{\alpha}^1, C_{\alpha}^2, C_{\beta}^1, C_{\beta}^2)$. The monodromy matrix $\rho(\gamma_{0-4})$ is trivial on the 2-cycles in the visible E_6 and hidden E_8 . Similarly, the monodromy for γ_{0-5} is given by

$$\begin{aligned}\tilde{C}_{A65} &= C_{A65}, & \tilde{C}_{A76} &= C_{A76} + C_{-\theta} - C_{\alpha}^1 + C_{\beta}^1, \\ \tilde{C}_{\alpha}^1 &= C_{\alpha}^1, & \tilde{C}_{\alpha}^2 &= C_{\alpha}^2 + C_{\alpha}^1 - C_{\beta}^1 - C_{-\theta}, \\ \tilde{C}_{\beta}^1 &= C_{\beta}^1, & \tilde{C}_{\beta}^2 &= C_{\beta}^2 - C_{\alpha}^1 + C_{\beta}^1 + C_{-\theta},\end{aligned}\tag{47}$$

and, finally, the one for γ_{0-6} is

$$\begin{aligned}\tilde{C}_{A65} &= C_{A65}, & \tilde{C}_{A76} &= C_{A76} + C_{-\theta} - C_{\beta}^1, \\ \tilde{C}_{\alpha}^1 &= C_{\alpha}^1, & \tilde{C}_{\alpha}^2 &= C_{\alpha}^2, \\ \tilde{C}_{\beta}^1 &= C_{\beta}^1, & \tilde{C}_{\beta}^2 &= C_{\beta}^2 + C_{\beta}^1 - C_{-\theta}.\end{aligned}\tag{48}$$

The 2-cycles inside the E_8 root lattice and $C_{\alpha,\beta}^{1,2}$ are mixed up under the monodromy $\rho(\gamma_{0-4,5,6})$. This clearly shows that the loops $\gamma_{0-4,5,6}$ are not homotopic to the loops that stay within the 8D gauge theory region of the moduli space. More importantly, $\rho(\gamma_{0-4,5,6})$ should be added to the list of generators of the full monodromy group; the full monodromy group is no longer the product of the $SU(3)_{\text{str}}$ Weyl group S_3 on the visible E_8 and something acting on the four 2-cycles $C_{\alpha,\beta}^{1,2}$, but the full monodromy group is larger¹² than that.

¹² The only non-vanishing entries in the 4th and 6th rows of the monodromy matrices (45–48) are in the 4th and 6th column, respectively, and are all “1”. This is an artifact of restricting the moduli space to the scaling region with $|\epsilon_{\eta}| \ll 1$. The period integrals over $C_{\alpha,\beta}^2$ are large and those for others small for $|\epsilon_{\eta}| \ll 1$. This is why $C_{\alpha,\beta}^2$ cannot mix into other 2-cycles. See also the appendix B. When one considers the full monodromy group for a family without the restriction of $|\epsilon_{\eta}| \ll 1$, new generators will appear, and we expect that this special feature will disappear.

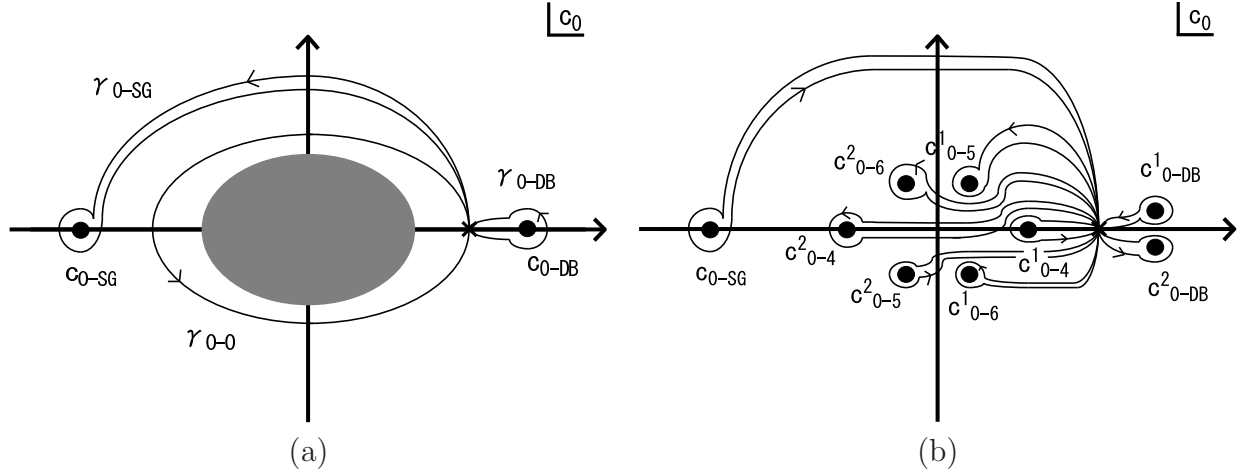


Figure 6: The monodromy locus appearing in the constant (c_1, c_2, g_0) slice of the moduli space, and non-trivial loops that go around them. We have chosen a slice that contains the base point (31). The panel (a) is a coarse picture based on $B_{\text{leading}} = 0$, where higher order corrections in ϵ_K are ignored. The three loops, γ_{0-DB} , γ_{0-SG} and γ_{0-0} stay within the 8D gauge theory region, away from the shaded region $|c_{0,*}| \lesssim \epsilon_K$. The panel (b) is a fine picture where higher order terms in ϵ_K are not dropped from $B = 0$. The $c_0 = 0$ monodromy point with the multiplicity 6 in $B_{\text{leading}} = 0$ (gray blob in the panel (a)) now splits into 6 distinct points; we can thus find six loops $\gamma_{0-4,5,6}^{1,2}$ in moduli space. The c_{0-DB} monodromy point with multiplicity 2 in the panel (a) also splits into two points $c_{0-DB}^{1,2}$, and two loops $\gamma_{0-DB}^{1,2}$ are found.

The subject of our real interest is the monodromy group of 2-cycles at the factorization limit (24–28). Although we have seen that the monodromy subgroup generated by loops in the constant (c_0, c_1, g_0) slice in the 8D gauge theory region is the \mathbb{Z}_2 subgroup of the Weyl group S_3 , there may be other generators in the full monodromy group, and the full monodromy group may be larger than \mathbb{Z}_2 . To find out candidates for such a generator, let us take a constant (c_1, c_2, g_0) slice of the moduli space and look at the complex c_0 plane.

The monodromy locus $B = 0$ in (38) should now be rewritten in terms of c_0, c_1, c_2 . At the leading order in ϵ_K , it becomes

$$B_{\text{leading}} = (c_0)^6 (4c_0c_2 - c_1^2)(c_0c_2 + c_1^2)^2, \quad (49)$$

and hence it appears as in Figure 6 (a). However, it was our motivation to study the geometry directly instead of gauge theory descriptions, to take account of higher order corrections in ϵ_K , and also to study the region with small c_0 . With all the higher order terms of $B = 0$

maintained, Figure 6 (b) is the precise picture of the monodromy locus appearing in the c_0 plane. It is important to note that the double point c_{0-DB} in Figure 6 (a) splits into two points, $c_{0-DB}^{1,2}$ in Figure 6 (b), due to the higher order terms in ϵ_K in $B = 0$. The split in the c_0 plane is approximately

$$\Delta c_{0-DB}^{1,2} = \pm \frac{\sqrt{3f}}{2} c_2 \sim \mathcal{O}(\epsilon_K^2 \epsilon_\eta^{\frac{1}{2}}), \quad (50)$$

which shows clearly that this is a higher order effect in ϵ_K . The split is certainly small, but still non-zero. Thus, the loops $\gamma_{0-DB}^{1,2}$ that go around either one of them can be separately non-trivial topologically in the moduli space; they may even become extra generators of the monodromy group. Each one of the $a_0 = a_{0-4,5,6}$ monodromy locus points in the a_0 plane (Figure 5) splits into a pair $c_{0-4}^{1,2}, c_{0-5}^{1,2}, c_{0-6}^{1,2} \sim \mathcal{O}(\epsilon_K \epsilon_\eta^{\frac{1}{2}})$ in the c_0 plane, because of the factorization condition (26). There are six loops $\gamma_{0-4,5,6}^{1,2}$ that go around them in the c_0 plane, and they might also generate extra monodromy of the 2-cycles.

We found by numerical study that the motion of 7-branes in the z plane along the loops $\gamma_{0-4,5,6}^{1,2}$ in the c_0 -plane is topologically the same¹³ as those along certain combinations of the loops $\gamma_{0-4,5,6}$ in the a_0 -plane. Thus, the monodromy of the loops $\gamma_{0-4,5,6}^{1,2}$ in the c_0 plane is given by

$$\begin{aligned} \rho(\gamma_{0-4}^1) &= \rho(\gamma_{0-4}), & \rho(\gamma_{0-4}^2) &= \rho(\gamma_{0-4}), \\ \rho(\gamma_{0-5}^1) &= \rho(\gamma_{0-5}), & \rho(\gamma_{0-5}^2) &= \rho(\gamma_{0-4})\rho(\gamma_{0-5})\rho(\gamma_{0-4})^{-1}, \\ \rho(\gamma_{0-6}^1) &= \rho(\gamma_{0-6}), & \rho(\gamma_{0-6}^2) &= \rho(\gamma_{0-4})^{-1}\rho(\gamma_{0-6})\rho(\gamma_{0-4}). \end{aligned} \quad (51)$$

This clearly shows that the loops digging into the $c_0 \simeq 0$ region give rise to monodromy of 2-cycles that have not been observed in the gauge theory descriptions on 7+1 dimensions; 2-cycles within the visible E_8 and those that are not are mixed up under the monodromy (51).

An $U(1)$ symmetry that survives all these monodromies correspond to a six-component row vector that remain invariant after multiplying any one of these monodromy matrices (33, 51) from the right. There is none. We therefore conclude that the $U(1)$ symmetry remaining in the $S[U(2) \times U(1)]$ Higgs bundle compactification is broken in the full geometry of F-theory compactification that has a region with $c_0 = 0$ on S_{GUT} . The problem B is indeed a problem.

To determine the monodromy associated with the loops $\gamma_{0-DB}^{1,2}$, one only needs to note that the motion of 7-branes in the z plane along these loops are topologically the same as

¹³This is easily guessed by the map (26–28).

those along the loop γ_{0-out} in the a_0 -plane. Thus,

$$\rho(\gamma_{0-DB}^{1,2}) = \rho(\gamma_{0-out}) = W_{CA76}. \quad (52)$$

These loops generate monodromy of 2-cycles in the visible E_8 ; combining this new generator and the one (33) that we already know in the gauge theory description on 7+1 dimensions, the whole S_3 Weyl group is generated. We have thought that the monodromy of 2-cycles is reduced from S_3 to \mathbb{Z}_2 in the factorization limit of the spectral surface, but because of the ϵ_K -suppressed higher order terms that were simply ignored in the 8D gauge theory description, actually the monodromy is not reduced from S_3 . We conclude that there is no unbroken $U(1)$ symmetry with non-trivial components in the visible E_8 that survives the monodromy generated by both (33) and (52). The problem A is a problem indeed.

To summarize,¹⁴ the full monodromy group contains at least (33), (51) and (52) as generators, maybe more, when the spectral surface is in the factorization limit (26–28). There is no unbroken $U(1)$ symmetry with non-trivial components in the visible E_8 under the full monodromy group. Thus, we cannot expect an unbroken $U(1)$ symmetry in the low-energy effective theory in ruling out the dimension-4 proton decay operators.

3.5 Non-K3-fibred 4-fold X_4

We have so far used a Calabi–Yau 4-fold X_4 that is a K3-fibration on S_{GUT} . However, this is just for a concreteness. The monodromy analysis certainly needs to be phrased for individual cases for X_4 ’s that are not K3-fibration over S_{GUT} . But the essence of the problem A and

¹⁴ It is useful for sanity check to exploit the relations following from the homotopy equivalence of various loops in the moduli space, as we did in the (a_0, a_2) moduli space in section 3.3. In the (c_0, c_2) moduli space, we have relations

$$\gamma_{2-DB} \sim \gamma_{0-DB} \sim \gamma_{0-DB}^1 \circ \gamma_{0-DB}^2, \quad (53)$$

$$\gamma_{2-SG} \sim \gamma_{0-SG}, \quad (54)$$

$$\gamma_{0-6} \circ \gamma_{0-4} \circ \gamma_{0-5} \sim \gamma_{0-\theta}, \quad (55)$$

$$\gamma_{0-6}^1 \circ \gamma_{0-5}^2 \circ \gamma_{0-4}^1 \circ \gamma_{0-4}^2 \circ \gamma_{0-6}^2 \circ \gamma_{0-5}^1 \sim \gamma_{0-0}. \quad (56)$$

Our results in section 3.2 and (52) both consistently yield $[W_{CA76}]^2 = [\rho(\gamma_{2-1})]^2$ in (53). Direct computation of $\rho(\gamma_{0-SG})$ indeed turned out to be the same as ρ_{2-SG} in (33). The homotopy relation (55) in the monodromy matrices is confirmed directly by using the results (45–48) and that in footnote 11. Finally, the product of (51) in the order specified in the left-hand side of (56) becomes $[\rho(\gamma_{0-6})\rho(\gamma_{0-4})\rho(\gamma_{0-5})]^2$, which is equal to $[\rho(\gamma_{0-\theta})]^2$, because of (55). This should be the same as $\rho(\gamma_{0-0})$, because the loop γ_{0-0} in the c_0 plane is mapped to $\gamma_{0-\theta} \circ \gamma_{0-\theta}$ in the a_0 plane through (26). All these consistency checks as a whole provides confidence in the results of our calculation.

B, and the essence of analysis remain the same. Let us take simplest non-K3 fibered models as examples: $B_3 = \mathbb{P}^3$, and S_{GUT} is a quadratic ($d = 2$) or cubic ($d = 3$) surface of B_3 , the models discussed in [12]. First, A_k in (2) are set to be [28]

$$A_k = s^{k-1} \tilde{A}_k, \quad \tilde{A}_k \in \Gamma(B_3; \mathcal{O}_{B_3}(-kK_{B_3} - (k-1)S_{GUT})), \quad (57)$$

where s is a global holomorphic section of $\mathcal{O}_{B_3}(S_{GUT}) \simeq \mathcal{O}_{\mathbb{P}^3}(dH)$ whose zero locus is the GUT divisor S_{GUT} . a_{6-k} on S_{GUT} in (3) correspond to $\tilde{A}_k|_{S_{GUT}}$. Suppose that a point $p_0 \equiv [0 : 0 : 0 : 1] \in \mathbb{P}^3$ is not contained in S_{GUT} . The base manifold except this point, $\mathbb{P}^3 \setminus p_0$ is covered by three patches $\simeq \mathbb{C}^3$, which constitute $\mathcal{O}_{\mathbb{P}^2}(1)$. Restriction of the original elliptic fibration over $B_3 = \mathbb{P}^3$ to that over $\mathcal{O}_{\mathbb{P}^2}(1)$, combined with a projection $\pi_0 : \mathcal{O}_{\mathbb{P}^2}(1) \rightarrow \mathbb{P}^2$ defines a complex surface fibration

$$\pi_0 \circ \pi_X : \pi_X^{-1}(\mathcal{O}_{\mathbb{P}^2}(1)) \rightarrow \mathbb{P}^2. \quad (58)$$

The fiber of this map is an elliptic fibration over \mathbb{C} , with 48 discriminant points on the \mathbb{C} plane. Although the number of $[p, q]$ 7-branes is not the same as in the case of an elliptic K3 manifold, independent topological 2-cycles and their intersection form of the fiber complex surface can be worked out by using the techniques in [29, 17]. Monodromy can be studied for loops¹⁵ in \mathbb{P}^2 . When $d \neq 1$, other points p_i 's in $B_3 = \mathbb{P}^3$ should also be chosen so that the analysis for $\pi_i : \mathbb{P}^3 \setminus p_i \simeq \mathcal{O}_{\mathbb{P}^2}(1) \rightarrow \mathbb{P}^2$ is carried out and all the ramification locus of the projection $\pi_i|_{S_{GUT}} : S_{GUT} \rightarrow \mathbb{P}^2$ is covered by some of the analysis of $\mathbb{P}^3 \setminus p_i$. Generalization from these examples to, e.g., toric B_3 (c.f. [30]), is straightforward.

The problem A arises from the difference between $a_{6-k} = \tilde{A}_k|_{S_{GUT}}$ and \tilde{A}_k , and the problem B arises essentially because of the local behavior of 2-cycles wherever a_0 vanishes. Thus, we expect similar phenomena also in the case of $B_3 = \mathbb{P}^3$, though we have not done the analysis. Since more than one points of S_{GUT} are projected onto the same point in \mathbb{P}^2 for $d \neq 1$, 2-cycles in E_8 on a point of S_{GUT} may mix with 2-cycles in E_8 on another point of S_{GUT} in the context of problem B.

¹⁵Since $\pi_0|_{S_{GUT}} : S_{GUT} \rightarrow \mathbb{P}^2$ is a d -fold covering, one can pull-back the complex-surface fibration (58) from \mathbb{P}^2 to S_{GUT} . The monodromy analysis can then be phrased for loops in S_{GUT} .

4 Consequences in Physics

4.1 U(1) Violating State-Mixing and Trilinear Couplings

We have studied a model of $E_8 \rightarrow E_6$ symmetry breaking with a spectral surface in the 2+1 factorization limit in the previous section, as a toy model of $E_8 \rightarrow \text{SU}(5)_{\text{GUT}}$ symmetry breaking in a certain factorization limit. On the contrary to the expectation in gauge theory in 7+1 dimensions, the study shows that there is no monodromy-invariant 2-cycle, and hence there is no unbroken U(1) symmetry in the low-energy effective theory below the Kaluza-Klein scale. Without an unbroken U(1) symmetry, we generally expect that dimension-4 proton decay operators will be generated. In this section, we discuss whether the dimension-4 proton decay operators are really generated from known interactions in string theory.

In F-theory, charged matter fields come from the degree of freedom of M2-branes wrapping on the 2-cycles corresponding to the representation of charged matters. Trilinear interactions are (likely to be) generated, if the sum of 2-cycles for the three fields is topologically trivial. Thus, by using this criterion, we can check whether dimension-4 proton decay operators are generated or not.

In the $E_8 \rightarrow E_6$ symmetry breaking model with the 2+1 factorization, the matter curve for E_6 -**27** representation splits into two irreducible pieces; one is characterized by $c_2 = 0$, and the other by $d_1 = -c_1 = 0$. Based on the gauge theory description on S_{GUT} , one would expect that the charged matter fields in the $E_6 \times \text{U}(1)$ -**27**₊₁ representation are localized along the $c_2 = 0$ curve in S_{GUT} , and those in the **27**₋₂ along the $c_1 = 0$ curve. Ignoring the monodromy that we studied in section 3.4, the 2-cycle $(C_{A76} + C_{A65})$ vanishes along the $c_1 = 0$ curve, while either C_{A65} or $(C_{-\theta} + C_{A76} + C_{A65})$ does along $c_2 = 0$. $4c_0c_2 - c_1^2 = 0$ is the ramification locus of the 2-fold spectral cover, where monodromy $W_{C_{A76}+C_{-\theta}}$ exchanges C_{A65} and $(C_{-\theta} + C_{A76} + C_{A65})$. See Figure 7. The trilinear interaction $\Delta W = \mathbf{27}_{+1} \cdot \mathbf{27}_{+1} \cdot \mathbf{27}_{-2}$ is generated at E_8 singularity enhancement points $c_1 = c_2 = 0$, because all the three 2-cycles vanish simultaneously there, and they satisfy

$$(C_{-\theta} + C_{A76} + C_{A65}) + C_{A65} + (C_{A76} + C_{A65}) \equiv 0 \pmod{E_6}. \quad (59)$$

This Yukawa coupling is invariant under the U(1) symmetry.

We know, however, that there are more monodromy among the 2-cycles. Under the monodromy (52), the 2-cycle C_{A65} for **27**₊₁ turns into $(C_{A76} + C_{A65})$ for **27**₋₂ and vice versa. The matter fields in the E_6 -**27** representation cannot remain pure eigenstates of the U(1) symmetry. This mixing among states with different U(1) charges (and hence the monodromy)

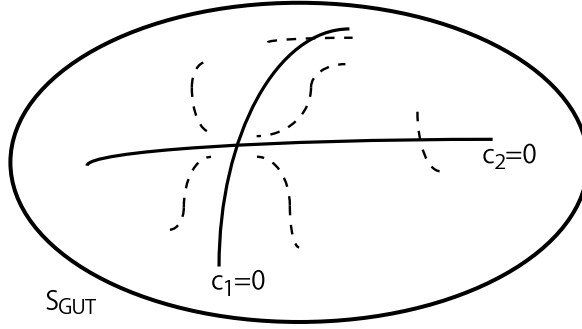


Figure 7: A schematic picture of matter curves and monodromy loci on S_{GUT} . The ramification locus $c_1^2 - 4c_2c_0 \simeq 0$ and a locus $(2c_1^2 + c_2c_0) \simeq 0$ with multiplicity 2 both approach the points of enhanced E_8 singularity. The multiplicity-2 branch, however, has a small split, and consists of two branches with multiplicity 1. Furthermore, all the three branches form a single irreducible component monodromy locus $B = 0$ around $(c_1, c_2) \simeq (0, 0)$. The monodromy locus $B = 0$ also intersect the matter curves at $(c_1, c_0) \simeq (0, 0)$ and $(c_2, c_0) \simeq (0, 0)$.

takes place around the monodromy locus

$$(c_{0,*})^4(c_{0,*}c_{2,*} + 2c_{1,*}^2)^2 \simeq 12f_0(\epsilon_K)^4(c_{1,*}^2)^4, \quad (60)$$

which is a part of $B = 0$ locus, just like the ramification locus $4c_0c_2 - c_1^2 \simeq 0$. Since this branch also approach the $c_1 = c_2 = 0$ point just like the ramification locus (see Figure 7), we do not have a reason to believe that the mixing (monodromy) due to this branch cancels, while that of the ramification locus remain. The mixing may be suppressed by some function of ϵ_K , but we cannot take ϵ_K to be literally zero in (5, 6, 15, 29) in $SU(5)_{GUT}$ models. Therefore, all sorts of $U(1)$ violating trilinear interactions $\Delta W = \mathbf{27} \cdot \mathbf{27} \cdot \mathbf{27}$ will be generated, unless there is a cancellation.

There are other groups of regions in S_{GUT} where the matter curves $c_1 = 0$ or $c_2 = 0$ encounters the $B = 0$ monodromy locus. One is $c_0 \simeq 0$ on $c_1 \simeq 0$ ($c_{2,*} \neq 0$), and the other is $c_0 \simeq 0$ along $c_2 \simeq 0$ ($c_{1,*} \neq 0$). The monodromy we studied in section 3.4 is relevant to the latter. The 2-cycle $(C_{-\theta} + C_{A76} + C_{A65})$ for $\mathbf{27}_{+1}$ and $(C_{A76} + C_{A65})$ for $\mathbf{27}_{-2}$ are exchanged under the monodromy (51) modulo 2-cycles $C_{\alpha,\beta}^{1,2}$. Thus, the “ $\mathbf{27}_{+1}$ ” fields will have non-vanishing $[C_{A76} + C_{A65}] \pmod{C_{\alpha,\beta}^{1,2}}$ component and vice versa. The mixing, however, will presumably be suppressed exponentially, because it is 2-cycles of finite size, rather than vanishing 2-cycles, that are exchanged under the monodromy at $c_0 \simeq 0$.

The $U(1)$ symmetry violating Yukawa couplings $\mathbf{27} \cdot \mathbf{27} \cdot \mathbf{27}$ are generated only when the

sum of three topological 2-cycles vanish in $H_2(\text{K3}; \mathbb{Z})$, just like in (59). Thus, just a single monodromy out of (51) acting on $(C_{-\theta} + C_{A76} + C_{A65})$ does not generate such a U(1) violating coupling **27**;

$$(C_{-\theta} + C_{A76} + C_{A65}) + C_{A65} + (\tilde{C}_{-\theta} + \tilde{C}_{A76} + \tilde{C}_{A65}) \neq 0 \quad (61)$$

in $H_2(\text{K3}; \mathbb{Z}) \pmod{E_6}$. After exploiting all the monodromies available in a 4-fold X_4 that is a K3 fibration on S_{GUT} ,¹⁶ however, all $C_{\alpha,\beta}^{1,2}$ will be mixed up and twisted over S_{GUT} , and eventually such a U(1) violating coupling will be generated, although the coupling constant may be highly suppressed. In the case of non-K3 fibred X_4 , $H_2(\text{K3}; \mathbb{Z})$ just has to be replaced by H_2 of the complex-surface fibration of (58).

The renormalizable proton decay operators are not the only consequence of the U(1) symmetry-breaking state mixing. Factorized spectral surface limit has been used for dimension-5 proton decay problem [11], or for the purpose of exploiting [31, 32] the idea of flavor structure in [33, 7, 8, 34]. The discussion so far implies that it is impossible to confine $\bar{\mathbf{5}}_H$ and $\mathbf{5}_H$ to separate irreducible pieces of $\text{SU}(5)_{\text{GUT}}$ matter curves completely. This may not be a big problem, as opposed to the dimension-4 proton decay problem, however, because the dimension-5 proton decay problem only requires a small amount of suppression; complete separation is not necessary. In the context of flavor structure of Yukawa couplings, the three copies of the visible sector matter fields $\bar{\mathbf{5}}_M$ or $\mathbf{10}_M$ may not be able to have wavefunctions strictly in a single irreducible component of the factorized matter curves, even at the factorization limit of the spectral surface. This means that the up-type Yukawa matrix of the low-energy effective theory below the Kaluza–Klein scale receives contributions from more than one point of enhanced E_6 singularity [31, 32]. If the state mixing is small, then this mixing is not terribly bad, and may even contribute in generating smaller eigenvalues; the flavor structure generated in this way is not necessarily similar to the one we observe in the Standard Model, however.

It should be remembered, however, that our analysis employed a 2+1 factorization in the $E_8 \rightarrow E_6$ symmetry breaking. Thus, it will not be a terribly bad guess to expect similar results for the 4+1 and 3+2 factorization in the $E_8 \rightarrow \text{SU}(5)_{\text{GUT}}$ symmetry breaking [10, 6, 11]. When another type of factorization (or monodromy subgroup of S_5) is employed, as in [14, 15], separate study is necessary, especially because it is not clear how the problem A will look like in such a factorization limit.

¹⁶Note, for example, that both f_0 and g_0 vanish at some points on S_{GUT} , where one cannot say ϵ_η is small. Although we did not study monodromy associated with non $|\epsilon_\eta| \ll 1$ region, generically we should expect such a monodromy in a compact model.

4.2 Loopholes in This Argument

The discussion so far hints that the dimension-4 proton decay operators are generated in the factorized spectral surface scenario. There are some loopholes in the argument, however. At the end of this article, here, we list up some loopholes that come to our minds. The list can also be taken as possible ways to save the factorized spectral surface solution.

First of all, the argument so far only showed that

- there is no unbroken $U(1)$ symmetry (apart from exceptional cases that we discuss later) in the low-energy effective theory that we hope would exclude the dimension-4 proton decay operators, and
- the picture of interactions as recombination of M2-branes without a change in the total topology does not exclude the $U(1)$ violating operators.

It is not that we have calculated the coefficients of such operators, and in fact, we do not even have a theoretical framework to calculate the coefficients within F-theory. A gauge theory on 7+1 dimensions cannot handle this. A possible direction is to exploit the Type IIB–M-theory duality or F-theory–Heterotic duality; dual descriptions may be used to see whether cancellation mechanism is likely to exist, or to make an estimate of the coefficients. That will tell us how small ϵ_K should be. Such a study is beyond the scope of this article, however.

If one literally sets $\epsilon_K = 0$, instead of fine-tuning it to be sufficiently small, then S_{GUT} becomes a locus of E_8 singularity. If a vector bundle on S_{GUT} has a structure group that is smaller than $SU(5)_{\text{str}} \times U(1)_Y$ so that an extra $U(1)$ factor is contained, then an unbroken $U(1)$ symmetry remains in the low-energy effective theory and prevent proton decay. The chirality of various charged matter fields in this case, however, are determined simply by intersection numbers of first Chern classes of those bundles and $K_{S_{GUT}}$ [10, 2, 3, 24], and existence of exotics is predicted easily [10, 12, 11]. It is also obvious that theories of flavor structure like those in [4, 33, 35, 7, 31, 32] are not applied to such a case, because only A_4 singularity is assumed along S_{GUT} .

Secondly, one will notice that our analysis in section 3 is based on a choice (26–28) of the solution to (25). The condition (25), however, can be solved in the form of

$$c_0 = ps, \quad d_1 = -qr, \quad c_1 = pr, \quad d_0 = qs \quad (62)$$

for some global holomorphic sections

$$s \in \Gamma(S_{GUT}; \mathcal{O}_S(\eta_0)), \quad p \in \Gamma(S_{GUT}; \mathcal{O}_S(\eta'_1)), \quad q \in \Gamma(S_{GUT}; \mathcal{O}_S(\eta'_2)), \quad (63)$$

$$r \in \Gamma(S_{GUT}; \mathcal{O}_S(\eta_0 + K_{S_{GUT}})); \quad (64)$$

here, $\eta'_{1,2}$ and η_0 are some divisors on S_{GUT} , and $c_2 \in \Gamma(S_{GUT}; \mathcal{O}_S(\eta'_1 + \eta_0 + 2K_{S_{GUT}}))$. What we studied in section 3 is the monodromy associated with $s = 0$ locus.

What if the global section s does not have a zero locus? This is possible if the line bundle $\mathcal{O}_S(\eta_0)$ is trivial; s can now take a constant non-zero value over the entire S_{GUT} . Suppose that this topological condition is satisfied. If we further assume that the divisor $K_{S_{GUT}}$ is not effective, as in del Pezzo surfaces and Hirzebruch surfaces, then there is no non-trivial global holomorphic section r . We have to set $r = 0$. This means that

$$c_1 = d_1 = 0 \quad (65)$$

over the entire S_{GUT} , which is nothing but the case we already listed as the rank-5 GUT scenario (ii) in Introduction. The dimension-4 proton decay problem can be solved completely in this scenario, because of an unbroken (or spontaneously broken) $U(1)$ symmetry in the low-energy effective theory; an extra 2-cycle is along S_{GUT} , and a semi-local geometry of this form along S_{GUT} is sufficient in ensuring the proton stability [10]. The singularity along S_{GUT} is either D_5 or A_5 in this case, and theories of flavor structure [4, 33, 35, 7, 31] are not applied here. Exotic-matter free conditions have also been studied for rank-5 GUT scenarios [12, 36].

If the divisor $K_{S_{GUT}}$ is effective, on the other hand, we can introduce a different set of topological conditions: all of line bundles $\mathcal{O}_S(\eta_0)$ and $\mathcal{O}_S(\eta'_{1,2})$ are trivial, so that there is no zero locus in s , p and q . This is possible for an effective $K_{S_{GUT}}$, because the matter curves belong to topological classes of effective divisors. Now there is no $a_0 = 0$ locus, and at least the problem B is gone, under this set of topological conditions.

An obvious loophole in the argument that follows (7) is that the coefficient of the highest degree term a_{5-k} may not have a zero locus. We have already exploited a case that a_0 is constant and non-zero, and a remaining alternative is a case¹⁷ where a_2 is constant and non-zero everywhere on S_{GUT} . This is possible only when $K_{S_{GUT}}$ is effective on S_{GUT} , and

¹⁷ As an example, one can consider an elliptic fibration $\pi_X : X_3 \rightarrow B_2 = \mathbb{P}^2$, and take S_{GUT} to be the zero locus of a homogeneous function s of degree 4 on $B_2 = \mathbb{P}^2$. The line bundle for \hat{A}_4 is trivial on B_2 , and hence $a_2 = \hat{A}_4|_{S_{GUT}}$ has to be constant on S_{GUT} . One will also see that $\hat{A}_6 = 0$ everywhere on B_2 . The divisor $K_{S_{GUT}}$ on S_{GUT} is effective.

$a_0 \in \Gamma(S_{GUT}; \mathcal{O}_S(-2K_{S_{GUT}}))$ vanishes as a consequence. An E_7 gauge theory¹⁸ is well-defined over the entire $S_{GUT} \times \mathbb{R}^{3,1}$. There is no mixing between 2-cycles in E_7 and those outside, and the problem B is gone in this case. What is more intriguing in this model is that there is no need to impose a factorization condition like (24) by hand. The commutant of $SU(5)_{GUT}$ in E_7 is $U(3)$. The decomposition

$$\begin{aligned} \text{Res}_{U(3) \times SU(5)_{GUT}}^{E_7} \mathbf{adj}. &= (\mathbf{adj}. , \mathbf{1}) + (\mathbf{1}, \mathbf{adj}.) \\ &+ [(\mathbf{3}, \overline{\mathbf{10}}) + (\wedge^2 \mathbf{3}, \mathbf{5}) + (\wedge^3 \mathbf{3}, \bar{\mathbf{5}})] + \text{h.c.} \end{aligned} \quad (66)$$

shows that there are two different kinds of charged matter fields in the $SU(5)_{GUT} \text{-}\bar{\mathbf{5}}$ representation. For a fully generic 3-fold spectral cover globally defined on S_{GUT} , $(\mathbf{3}, \overline{\mathbf{10}}) + (\bar{\mathbf{3}}, \mathbf{10})$ matter fields are localized along the $a_5 = 0$ locus, while $(\wedge^2 \mathbf{3}, \mathbf{5}) + \text{h.c.}$ and $(\wedge^3 \mathbf{3}, \bar{\mathbf{5}}) + \text{h.c.}$ matter fields are localized along the $(-a_2 a_5 + a_4 a_3) = 0$ and $a_3 = 0$ loci, respectively. This factorization / decomposition automatically takes place under this topological condition.¹⁹ Because of the commutation relation of the E_7 Lie algebra, $(\wedge^2 \mathbf{3}, \mathbf{5})$ is identified with the origin of the up-type Higgs multiplet. If $(\wedge^3 \mathbf{3}, \bar{\mathbf{5}})$ and $(\wedge^2 \bar{\mathbf{3}}, \bar{\mathbf{5}})$ are identified with $\bar{\mathbf{5}}_H$ and $\bar{\mathbf{5}}_M$, respectively,²⁰ then the moduli $(\mathbf{adj}. , \mathbf{1})$ for the $U(3)$ spectral surface may become right-handed neutrinos [14, 6]. The up-type Yukawa couplings and down-type/charged lepton Yukawa couplings originate from

$$\Delta W = (\wedge^4 \mathbf{8})^{MNPQ} \cdot \mathbf{adj}.^I{}_H \cdot (\wedge^4 \mathbf{8})^{HJKL} \epsilon_{IJKLMNPQ} \quad (67)$$

in the language of $\mathfrak{su}(8) \subset \mathfrak{e}_7$, and the neutrino Yukawa couplings from [10]

$$\Delta W = \text{tr}_{\mathfrak{su}(8)} (\mathbf{adj}. , [\mathbf{adj}. , \mathbf{adj}.]) . \quad (68)$$

It is worthwhile to study the monodromy for this case, e.g, using the example in footnote 17, to see how the problem A will look like, because the “problem A” may be quite different in nature, or may even be absent, in such a case without a need for imposing factorization condition by hand.

¹⁸ E_7 is a minimal choice in obtaining all the matter fields and their trilinear interactions of the supersymmetric standard Models [10, 37, 15]. Thus, it is not an option for realistic GUT models to assume that a_3 is constant and non-zero over S_{GUT} .

¹⁹We thank Cumrun Vafa for discussion.

²⁰The exotic free condition and successful doublet–triplet splitting cannot be realized simultaneously in this identification, however [11]. If the two components are identified in the opposite way with $\bar{\mathbf{5}}_H$ and $\bar{\mathbf{5}}_M$, the interaction (68) gives rise to the trilinear interaction $\Delta W = S \bar{\mathbf{5}}_H \mathbf{5}_H$ of the next-to-minimal supersymmetric Standard Models, and a candidate for the right-handed neutrinos is lost.

Finally, there are also loopholes that resort to continuous fine-tuning of complex structure parameters. Flux compactifications should ultimately explain such a tuning. At the level of gauge theory description on 7+1 dimensions, we introduced a parametrization of the complex structure moduli a_0 , a_2 and a_3 by $c_{0,1,2}$ as in (26–28), so that the spectral surface factorizes in the new parametrization. But the ultimate goal is to reduce the monodromy of 2-cycles so that an unbroken $U(1)$ symmetry is maintained in the low-energy effective theory.²¹ Thus, the generalized version of the solution is to consider a parametrization of the complex structure moduli $(a_{0,2,3}, f_0, g_0, a_0'')$ of X_4 so that the polynomial B in (38) is factorized appropriately in the new parameters. The geometry for compactification should be given by holomorphic sections from S_{GUT} to the new parameter space. It will be straightforward to work out the expression for “ B ” in the case of $E_8 \rightarrow SU(5)_{GUT}$ symmetry breaking.

In the case of $E_8 \rightarrow E_6$ symmetry breaking, the polynomial B should be factorized so that the split between $c_{2-DB}^1 c_{0-DB}^1$ and $c_{2-DB}^2 c_{0-DB}^2$ disappears and they form a monodromy locus of multiplicity 2. The monodromy (52) is gone in this limit; this is a fine-tuning solution to the problem A.

A hint for a fine-tuning solution to the problem B comes from Heterotic dual description. In Heterotic string language, one can tune complex structure moduli so that the elliptic fibred Calabi–Yau 3-fold admits a non-trivial section; moduli of spectral surfaces of V_1 and V_2 may be tuned so that the line bundle $\det V_1$ corresponds to the non-trivial section.²² In other words, this is to consider the factorization limit of (93) instead of the factorization limit of (8, 10). There still remains a problem of determining the ϵ_η suppressed corrections, because the spectral surface picture relies on supergravity + $E_8 \times E_8$ super Yang–Mills approximation in the Heterotic description (see the appendix B for more). In F-theory language, this tuning, we expect, will correspond to factorization of B so that all the six branches $c_{0-4,5,6}^{1,2}$ somehow come on top of one another in the new parametrization space to form a monodromy locus of multiplicity 6. The monodromy, then, is $\rho(\gamma_{0-0})$, which we know is trivial on the E_8 part of the 2-cycle. We do not have a concrete picture of how to modify the parametrization (26–28) systematically to obtain the new parametrization, however.

²¹Strictly speaking, we do not need a full $U(1)$ symmetry, or equivalently a monodromy-invariant 2-cycle. If a torsion component survives the monodromy, then some selection rule will remain, as we discussed in section 4.1.

²²We thank Ron Donagi for discussion.

Acknowledgements

TW thanks Ron Donagi, Sergei Galkin, Joseph Marsano, Cumrun Vafa and Martijn Wijnholt for stimulating discussion, useful comments and communications. This work started when two of the authors (TK and TW) were staying at YITP, Kyoto University, during a program “Branes, Strings and Black Holes,” September–November, 2009. TW thanks Caltech theory group and KITP, UC Santa Barbara, for hospitality, where he stayed during the final stage of this project. This work was supported in part by JSPS Research Fellowships for Young Scientists (HH), by a Grant-in-Aid #19540268 from the MEXT of Japan (TK), by Global COE Program “the Physical Sciences Frontier”, MEXT, Japan (YT), by WPI Initiative, MEXT, Japan and by the NSF under Grant No. PHY05-51164 (TW).

A Some examples of computing the monodromy of 2-cycles

In sections 3.2–3.4, we need to study monodromy of 2-cycles of an elliptic fibered K3 manifold for loops in the moduli space of the elliptic K3; this monodromy group is used in this article, to find out whether an unbroken $U(1)$ symmetry remains in the effective theory and the dimension-4 proton decay operators (1) are ruled out. In order to calculate the monodromy of 2-cycles, we first need to identify 2-cycles in an elliptically fibered K3 surface that constitute a basis of $H_2(K3; \mathbb{Z})$. Second, we analyze the changes of the 2-cycles when we move along a loop in the moduli space.

We are not interested so much in the fiber class and base class of the elliptic fibration, because they do not correspond to a $U(1)$ vector field or a $U(1)$ symmetry. When an M2-brane is wrapped on one of other topological 2-cycles of an elliptic K3 manifold, it is interpreted as a string junction configuration on the base manifold \mathbb{P}^1 . The first task, therefore, is to identify “independent” string junction configurations, which has already been done completely in [17]. In section A.1, we briefly review the results of [17], while explaining details of our conventions that are used in the calculation in section A.2.

String junction configurations on \mathbb{P}^1 are easier to deal with (for string theorist) than topological 2-cycles in an elliptic K3 manifold. Thus, we calculate monodromy of topological 2-cycles by following the configuration of string junctions along a loop in the moduli space of the elliptic K3. We demonstrate the technique of the computation of the monodromy explicitly for some loops as examples in section A.2.

The appendix A constitutes nearly a third of this article, but it is a technical note in nature. The main text will be readable without reading the details of this appendix.

A.1 Independent 2-cycles in the language of string junctions

Let us consider a 7-brane configuration in a complex z plane, where $[1, 0]$ 7-branes (called A-branes), $[1, -1]$ 7-brane (called B-branes), $[1, 1]$ (C-branes) and $[3, -1]$ 7-branes (we call them “D”-branes) are line up from left to right as

$$A^8 BC^2 D A^8 BC^2 D, \quad (69)$$

and branch cuts run from all of those 7-branes to the infinity in the z -plane in the positive imaginary direction. This is the $\hat{E}_9 \hat{E}_9$ configuration in [17], which contains two sets of 7-brane configuration $[A^7 BC^2]$ for E_8 . We assign names to these 7-branes. The eight A-branes on the left are called $A8$ – $A1$ from left to right, and the two C-branes on the left called $C1$ and $C2$ from left to right (see Figure 1). The B-brane and “D”-brane on the left are simply called B and D . The twelve 7-branes on the right are named similarly, with an extra $'$, such as $A8'$, $A7'$ etc. We will see shortly that the configuration of $[p, q]$ 7-branes and branch cuts can be made topologically the same as this for an explicit choice of a base point in the elliptic K3 moduli space.

We have adopted a convention that a (p, q) string corresponds to an M2-brane wrapped on $(p\alpha + q\beta)$ cycle of the T^2 -fiber.²³ The (r, s) charge of a string undergoes the monodromy

²³Here, the topological 1-cycles of T^2 , α and β are assumed to have a intersection form $\langle \alpha, \beta \rangle = -\langle \beta, \alpha \rangle = 1$. This follows the convention of [38, 26]. References [39, 40, 17], on the other hand, define a (p', q') string as an M2-brane wrapping on $(p'\alpha - q'\beta)$ -cycle of a torus. While the (r, s) charge are re-labeled as in (72) in the convention of [38, 26] when crossing a cut of a $[p, q]$ 7-brane in an anti-clockwise direction, the

$$\begin{pmatrix} r' \\ s' \end{pmatrix} = \begin{pmatrix} 1 & 0 \\ 0 & -1 \end{pmatrix} \begin{pmatrix} r \\ s \end{pmatrix} \quad (70)$$

charge in the convention of [40, 17, 39] changes by the monodromy matrix given by

$$M'_{p', q'} \equiv \begin{pmatrix} 1 & 0 \\ 0 & -1 \end{pmatrix} M_{p=p', q=-q'} \begin{pmatrix} 1 & 0 \\ 0 & -1 \end{pmatrix} = \begin{pmatrix} 1 + p'q' & -p'^2 \\ q'^2 & 1 - p'q' \end{pmatrix} \quad (71)$$

when crossing a branch cut of a $[p', q']$ 7-brane in the anti-clockwise direction. Certainly the last expression of $M'_{p', q'}$ happens to look like an inverse matrix of $M_{p, q}$ with p and q simply replaced (not rewritten!) by p' and q' . But $M'_{p', q'}$ in (71) and $M_{p, q}$ in (72) should be regarded as physically equivalent $\text{SL}(2; \mathbb{Z})$ monodromy matrices in different conventions.

as in

$$\begin{pmatrix} r \\ s \end{pmatrix} \rightarrow M_{p,q} \begin{pmatrix} r \\ s \end{pmatrix} \equiv \begin{pmatrix} 1-pq & p^2 \\ -q^2 & 1+pq \end{pmatrix} \begin{pmatrix} r \\ s \end{pmatrix} \quad (72)$$

when the string crosses a branch cut for a $[p, q]$ 7-brane in anti-clockwise direction.

Any string junctions on \mathbb{P}^1 correspond to closed 2-cycles of an elliptic K3. We can pull out any junction configurations to the negative imaginary direction by continuous deformation, so that the configuration does not cross a branch cut; string creation process should be used if necessary. By deforming junction configurations in this way, we can express junction configurations by 24 integers N^i , where $i = A8, A7, \dots, A1, B, \dots, C1', C2', D'$ run over the twenty four 7-branes; N^i are the numbers of (p_i, q_i) strings coming out of the i -th 7-brane whose charge is $[p_i, q_i]$. For example, the junction configuration (and the 2-cycle) named C_{A76} is characterized by $N^{A7} = 1$, $N^{A6} = -1$, and $N^i = 0$ for all other 7-branes. C_{BCD} corresponds to $N^B = N^{C1} = N^{C2} = 1$, $N^D = -1$, and $N^i = 0$ for all the other 7-branes. See Figure 1. We denote 22 independent closed 2-cycles by [17]

- visible E_8 : $C_{A76} \sim C_{A21}, C_{ABC}$ and C_{C12} (see Figure 1),
- hidden E_8 : $C'_{A76} \sim C'_{A21}, C'_{ABC}$ and C'_{C12} that are the same string junction configuration as the corresponding ones in visible E_8 , except that their endpoints are on the 7-branes $A8'-A1', B', C1', C2'$ and D' ,
- others: $C_{A87}, C_{BCD}, C'_{A87}, C'_{BCD}, C_{AA'}, C_{DD'}$ (see Figure 1).

Among the 22 closed 2-cycles listed above, however, 2 linear combinations

$$C_{BCD} + C'_{BCD} \quad \text{and} \quad -C_{A87} + -C'_{A87} + C_{-\theta} + C'_{-\theta} \quad (73)$$

can be expressed as a boundary of 3-dimensional cells; here, $C_{-\theta}$ is defined by (12), and $C'_{-\theta}$ is its obvious ' version. We thus drop C'_{BCD} and $C'_{-\theta} - C'_{A87}$, and use $C_{BCD}, C_{-\theta}, C_{AA'}, C_{DD'}$ and the 16 2-cycles of the visible and hidden E_8 's as representatives²⁴ of the 20 independent topological 2-cycles in $H_2(\text{K3}; \mathbb{Z})$ [17].

For an appropriate choice of a basis of $H_2(\text{K3}; \mathbb{Z})$, the intersection form becomes [41]

$$-C(E_8) \oplus \begin{pmatrix} 0 & 1 \\ 1 & 0 \end{pmatrix} \oplus \begin{pmatrix} 0 & 1 \\ 1 & 0 \end{pmatrix} \oplus -C(E'_8), \quad (74)$$

²⁴ The homology group of a rational elliptic surface (also known as “ dP_9 ”) can be expressed in a similar manner. Any linear combinations of C_{BCD} and $C_{-\theta} - C_{A87}$ become the boundary, and hence $H_2(dP_9; \mathbb{Z})$ is generated by the eight visible E_8 2-cycles and the fiber and base classes. In the homology group of a rational elliptic surface, $[C_{A87}] = [C_{-\theta}]$. This relation, however, does not hold for an elliptic K3 manifold.

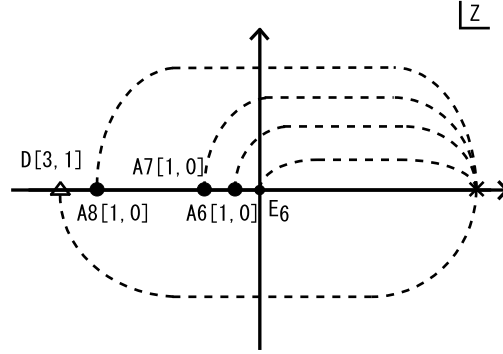


Figure 8: The 7-brane configuration at the base point (19). The dotted curves represent branch cuts. The approximate location of A6 7-brane is $z_{A6} \sim -\frac{27}{64} \frac{a_3^4}{a_2^3} \sim \mathcal{O}(\epsilon_K^6 \epsilon_\eta^1 \delta^4)$ and $z_{A7} \sim -\frac{4}{27} \frac{a_2^3}{a_0^2} \sim \mathcal{O}(\epsilon_K^6 \epsilon_\eta)$ for A7 7-brane [see also (34)]. A8 and D 7-branes are at $z \sim \mathcal{O}(\epsilon_\eta)$.

where $C(E_8)$ and $C(E'_8)$ denotes the Cartan matrix of $E_8^{(i)}$ respectively, with an extra 2 by 2 block for the fiber and base classes. The eight 2-cycles of the visible E_8 and those of the hidden E_8 can be used as the first and last eight elements of the basis. The remaining four elements of a basis for the intersection form above can be chosen as the following four linear combinations [17]:

$$C_\alpha^1 = -C_{A87} + C_{-\theta}, \quad C_\alpha^2 = -C_{A87} + C_{-\theta} + C_{AA'}, \quad (75)$$

$$C_\beta^1 = C_{BCD}, \quad C_\beta^2 = C_{BCD} + C_{DD'}. \quad (76)$$

$\langle C_\alpha^1, C_\alpha^2 \rangle = 1$, $\langle C_\beta^1, C_\beta^2 \rangle = 1$, and all other intersection numbers among the four 2-cycles vanish.

A.2 Some examples of the monodromy

A.2.1 The 7-brane configuration at the base point

In section A.2, we present the practical procedure of calculation of monodromy of 2-cycles for some loops in the moduli space of elliptic K3 manifold (11). We have chosen a base point as in (19) in the moduli space. The 7-branes configuration on the base \mathbb{P}^1 at this base point is shown in Figure 8. Since we introduced a small parameter δ in the definition of the base point, the elliptic K3 manifold for the base point must realize a hierarchical symmetry breaking $E_8 \rightarrow E_7 \rightarrow E_6$. We thus assign the name A6 to the 7-brane that is closest to the

E_6 point. The branch cuts and the $[p, q]$ charges of the 7-branes are given as in Figure 8. This arrangement is certainly the way anticipated in (69), but it is not trivial whether the cut configuration and charge assignment in the figure are correct for the specific choice of the complex structure at the base point. We confirmed that this is a right choice, by examining the 1-cycles of the T^2 fiber to degenerate and monodromy of the complex structure of the fiber at these 7-branes.

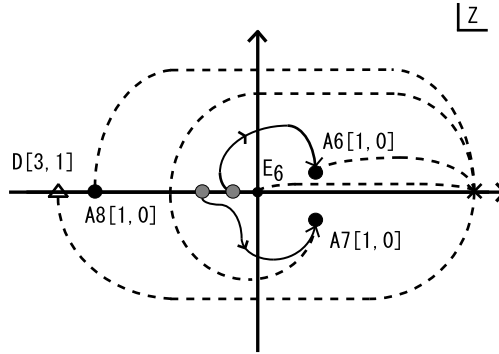
A.2.2 The Monodromy of the loop γ_{2-A}

First, we consider the monodromy around the loop γ_{2-A} . This loop goes around a triple point of the monodromy locus. The loop γ_{2-A} is depicted in the Figure 3. We decompose the loop γ_{2-A} into three paths in calculating the monodromy.

1. approaching $a_2 = a_{2-A}$ from the base point from the right (path 1),
2. going around $a_2 = a_{2-A}$ in the anti-clockwise direction (path 2), and finally,
3. going back to the base point from $a_2 = a_{2-A}$ (path 3).

The 2-cycles at the base point change when evaluated after they go along path 1, path 2 and path 3. We can read the monodromy matrix from the change of the 2-cycles.

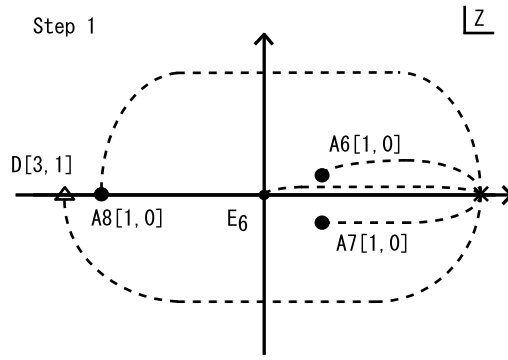
Path 1: The movement of 7-branes corresponding to the path 1 is shown in the first part of the Table 2. After completing the path 1, we rearrange the branch cuts as a preparation for the path 2, by two steps as in the second and third part of the Table 2. The changes of 2-cycles (string junction) as well as the change in the $[p, q]$ charges of various 7-branes during the rearrangement of the branch cuts are also shown in the table below the corresponding figures (Table 2). As we already explained in section A.1, string junction configurations are always deformed continuously so that they do not cross any one of branch cuts. The numbers in the table show the number of $[p_i, q_i]$ strings coming out of a $[p_i, q_i]$ 7-brane.



	A8 [1,0]	A7 [1,0]	A6 [1,0]	A5 [1,0]	A4-A1 [1,0]	B [1,-1]	C1,2 [1,1]	D[3,1]
C_{A76}	0	1	-1	0	0	0	0	0
C_{A65}	0	0	1	-1	0	0	0	0
C_{BCD}	0	0	0	0	0	1	1	-1

↓ step 1

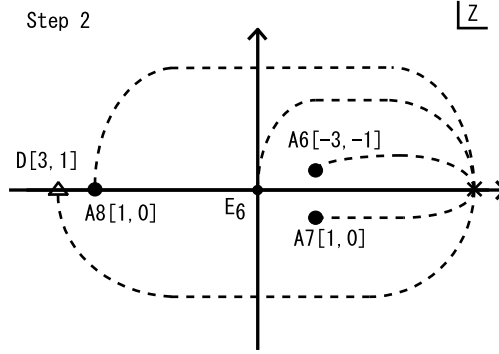
Passing $A6 + E_6$ 7-branes through
the branch cuts of $A7$ 7-branes from right to left.



	A8 [1,0]	A6 [1,0]	A5 [1,0]	A4-A1 [1,0]	B [0,-1]	C1,2 [2,1]	A7 [1,0]	D[3,1]
C_{A76}	0	-1	0	0	0	0	1	0
C_{A65}	0	1	-1	0	0	0	0	0
C_{BCD}	0	0	0	0	1	1	-1	-1

↓ step 2

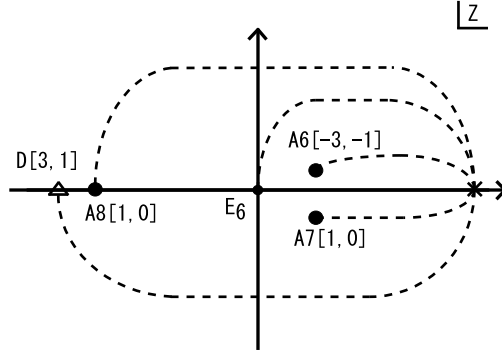
Passing $A6$ 7-branes through
the branch cuts of E_6 7-branes from left to right.



	A8 [1,0]	A5 [1,0]	A4-A1 [1,0]	B [0,-1]	C1,2 [2,1]	A6 [-3, -1]	A7 [1,0]	D[3,1]
C_{A76}	0	0	0	-1	-1	-1	1	0
C_{A65}	0	-1	0	1	1	1	0	0
C_{BCD}	0	0	0	1	1	0	-1	-1

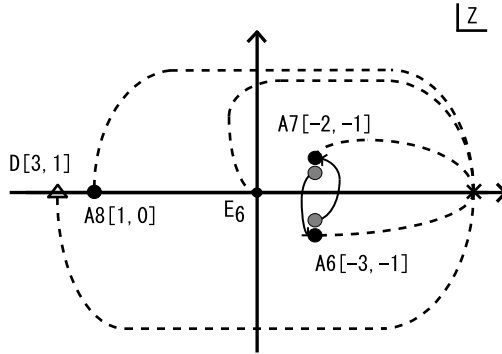
Table 2: The first figure shows the motion of 7-branes along the path 1. The location of 7-branes before the movement is depicted by the gray circles. The next two figures show how to rearrange branch cuts. The changes of 2-cycles (string junctions) of the process are shown below the corresponding figures. We denotes the $[p, q]$ charge next to the name of 7-branes.

Path 2: During the path 2, the $A6$ 7-brane and $A7$ 7-brane mutually rotate around the other by 3π , as in Table 3. We have rearranged the branch cuts at the end of path 1, so that they do not cross any branch cuts except the cuts of themselves. Note, however, that $A6$ and $A7$ 7-branes are not mutually local after the rearrangement of the branch cuts. Therefore we have to take a close look during the path 2 at the changes of $[p, q]$ charges of the $A6$ and $A7$ 7-branes, and at the changes of string junction configurations that have end points on $A6$ or $A7$. For every π rotation, either $A6$ or $A7$ has to cross the branch cut of the other. Thus, we need to trace the changes of junction configurations for every π rotation. Table 3 shows the results. From the Table 3, the 2-cycles do not change after the 3π rotation.



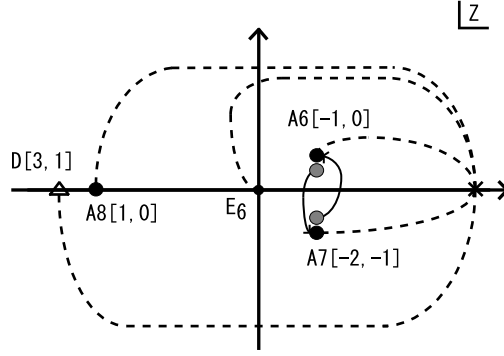
	A8 [1,0]	A5 [1,0]	A4-A1 [1,0]	B [0,-1]	C1,2 [2,1]	A6 [-3, -1]	A7 [1,0]	D[3,1]
C_{A76}	0	0	0	-1	-1	-1	1	0
C_{A65}	0	-1	0	1	1	1	0	0
C_{BCD}	0	0	0	1	1	0	-1	-1

$\downarrow [0 \rightarrow \pi \text{ rotation}]$



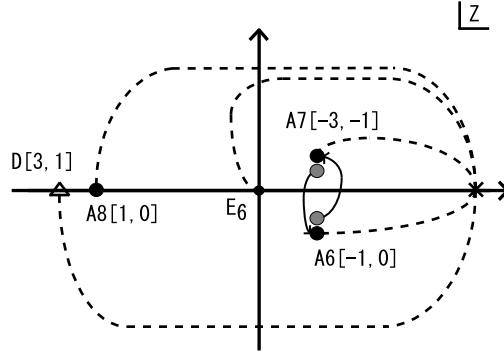
	A8 [1,0]	A5 [1,0]	A4-A1 [1,0]	B [0,-1]	C1,2 [2,1]	A7 [-2, -1]	A6 [-3,-1]	D[3,1]
C_{A76}	0	0	0	-1	-1	1	-2	0
C_{A65}	0	-1	0	1	1	0	1	0
C_{BCD}	0	0	0	1	1	-1	1	-1

$\downarrow [\pi \rightarrow 2\pi \text{ rotation}]$



	A8 [1,0]	A5 [1,0]	A4-A1 [1,0]	B [0,-1]	C1,2 [2,1]	A6 [-1, 0]	A7 [-2,-1]	D[3,1]
C_{A76}	0	0	0	-1	-1	-2	-1	0
C_{A65}	0	-1	0	1	1	1	1	0
C_{BCD}	0	0	0	1	1	1	0	-1

$\downarrow [2\pi \rightarrow 3\pi \text{ rotation}]$

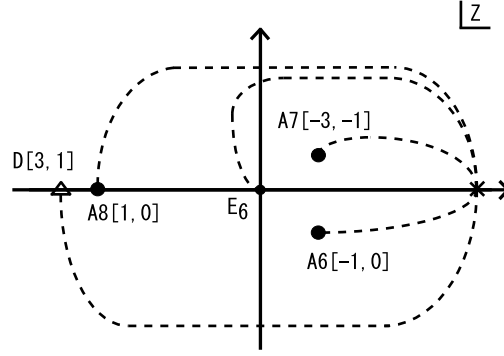


	A8 [1,0]	A5 [1,0]	A4-A1 [1,0]	B [0,-1]	C1,2 [2,1]	A7 [-3, -1]	A6 [-1,0]	D[3,1]
\tilde{C}_{A76}	0	0	0	-1	-1	-1	-1	0
\tilde{C}_{A65}	0	-1	0	1	1	1	0	0
\tilde{C}_{BCD}	0	0	0	1	1	0	1	-1

Table 3: The motion of 7-branes and the changes of the 2-cycles along the path 2. \tilde{C} s represent the 2-cycles after 3π rotation.

Path 3: The path 3 simply follows the path 1 in the opposite direction. Before going back to the base point, however, we rearrange the branch cuts in a backward direction of

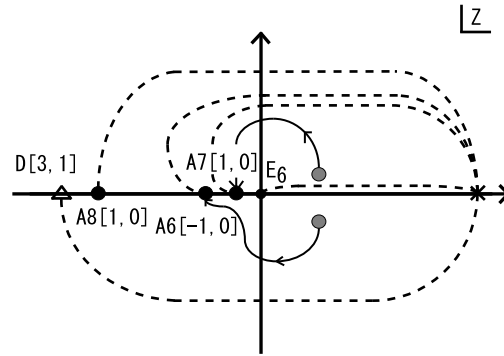
the Table 2 with $A6$ and $A7$ exchanged. After that, we go back to the base point along the path 3, and 7-branes move along the same path as in the first part of Table 2 in the opposite direction without crossing any branch cuts; this is depicted in the second part of the Table 4.



	A8 [1,0]	A5 [1,0]	A4-1 [1,0]	B [0,-1]	C1,2 [2,1]	A7 [-3, -1]	A6 [-1,0]	D[3,1]
\tilde{C}_{A76}	0	0	0	-1	-1	-1	-1	0
\tilde{C}_{A65}	0	-1	0	1	1	1	0	0
\tilde{C}_{BCD}	0	0	0	1	1	0	1	-1

↓

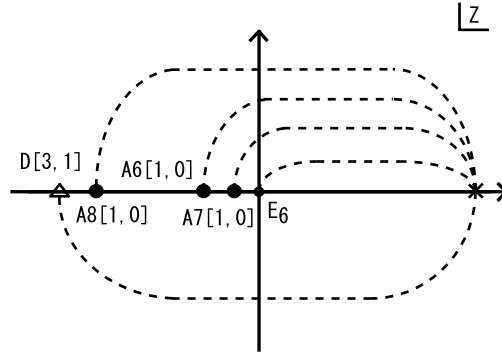
Rearrangement of branch cuts and going along the path 3.



	A8 [1,0]	A6 [-1,0]	A7 [1,0]	A5 [1,0]	A4-1 [1,0]	B [1,-1]	C1,2 [1,1]	D[3,1]
\tilde{C}_{A76}	0	-1	-1	0	0	0	0	0
\tilde{C}_{A65}	0	0	1	-1	0	0	0	0
\tilde{C}_{BCD}	0	0	0	0	0	1	1	-1

↓

Changing the bases into the ones before the rotation



	A8 [1,0]	A6 [1,0]	A7 [1,0]	A5 [1,0]	A4-1 [1,0]	B [1,-1]	C1,2 [1,1]	D[3,1]
\tilde{C}_{A76}	0	1	-1	0	0	0	0	0
\tilde{C}_{A65}	0	0	1	-1	0	0	0	0
\tilde{C}_{BCD}	0	0	0	0	0	1	1	-1

Table 4: The motion of 7-branes and the changes of 2-cycles along the path 3.

Comparing the first table of Table 2 with the last table of Table 4, we find that the 2-cycles do not change at the end of the whole process. Thus, the monodromy of the 2-cycles is trivial for the loop γ_{2-A} .

A.2.3 The Monodromy of the loop γ_{2-2}

Let us follow the motion of 7-branes when a_2 varies along the loop γ_{2-2} . First, let us separate the loop γ_{2-2} into three pieces;

1. a path from the base point to the right of a_{2-2} (path 1).
2. a loop around a_{2-2} (path 2).

3. a path which is the reverse of the first path (path 3).

When a_2 varies along the first path, 7-branes move as shown in Figure 9.

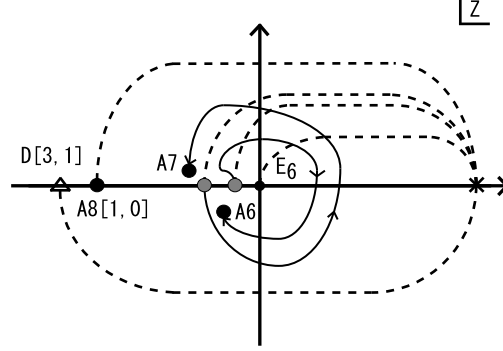
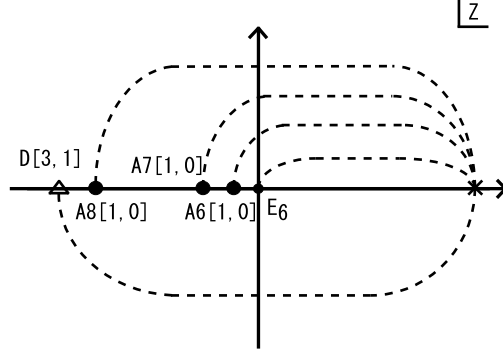


Figure 9: The motion of A6, A7 7-branes along the path 1. Since the motion of A8, D 7-branes are not relevant to the monodromy of this case, we do not write it in the figure.

When a_2 varies along the second path, the A6 7-brane's position and the A7 7-brane's position exchange with each other.

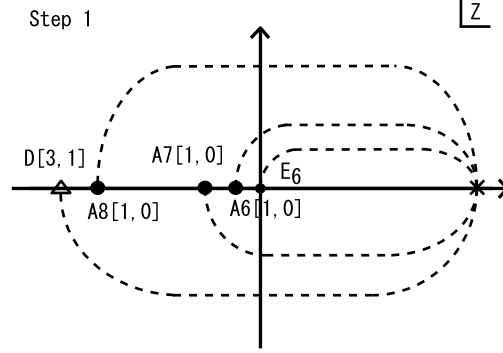
Next let us consider to rearrange the branch cuts of 7-branes before the exchange of A6 and A7 so that both 7-branes do not cross any branch cuts except for themselves' during the exchange. This process is collected in the Table 5. It shows that the configuration of 7-branes and how the 2-cycles change by the above rearrangement.



	A8[1,0]	A7[1,0]	A6[1,0]	A5[1,0]	A4-A1[1,0]	B[1,-1]	C1, C2[1,1]	D[3,1]
C_{A65}	0	0	1	-1	0	0	0	0
C_{A76}	0	1	-1	0	0	0	0	0
C_{A87}	1	-1	0	0	0	0	0	0
C_{BCD}	0	0	0	0	0	1	1	-1

↓ step 1

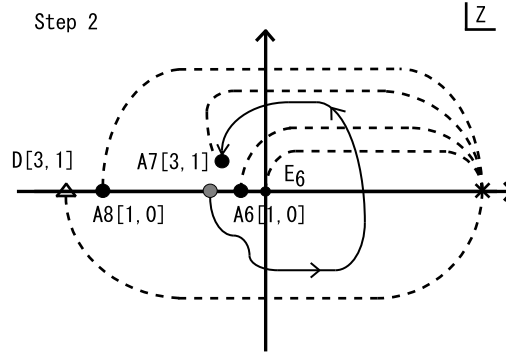
A6 and E_6 go across the cut of A7 from right to left



	A8[1,0]	A6[1,0]	A5[1,0]	A4-A1[1,0]	B[0,-1]	C1, C2[2,1]	A7[1,0]	D[3,1]
C_{A65}	0	1	-1	0	0	0	0	0
C_{A76}	0	-1	0	0	0	0	1	0
C_{A87}	1	0	0	0	0	0	-1	0
C_{BCD}	0	0	0	0	1	1	0	-1

↓ step 2

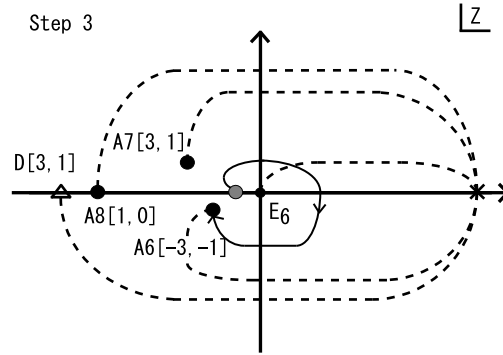
A7 goes across the cut of A6 and E_6 from right to left.



	A8[1,0]	A7[3,1]	A6[1,0]	A5[1,0]	A4-A1[1,0]	B[0,-1]	C1, C2[2,1]	D[3,1]
C_{A65}	0	0	1	-1	0	0	0	0
C_{A76}	0	1	-2	-1	-1	3	1	0
C_{A87}	1	-1	1	1	1	-3	-1	0
C_{BCD}	0	-1	1	1	1	-2	0	-1

↓ step 3

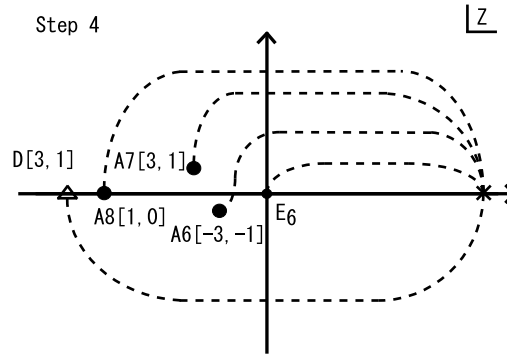
A6 goes across the cut of E_6 from left to right.



	A8[1,0]	A7[3,1]	A5[1,0]	A4-A1[1,0]	B[0,-1]	C1, C2[2,1]	A6[-3,-1]	D[3,1]
C_{A65}	0	0	-1	0	1	1	1	0
C_{A76}	0	1	-1	-1	1	-1	-2	0
C_{A87}	1	-1	1	1	-2	0	1	0
C_{BCD}	0	-1	1	1	-1	1	1	-1

↓ step 4

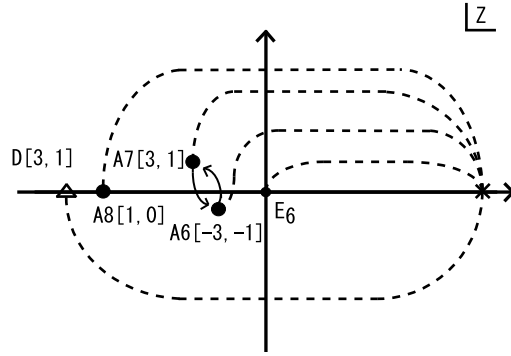
E_6 goes across the cut of A6 from left to right.



	A8[1,0]	A7[3,1]	A6[-3,-1]	A5[4,1]	A4-A1[4,1]	B[9,2]	C1, C2[-1,0]	D[3,1]
C_{A65}	0	0	1	-1	0	1	1	0
C_{A76}	0	1	-2	-1	-1	1	-1	0
C_{A87}	1	-1	0	1	1	-2	0	0
C_{BCD}	0	-1	1	1	1	-1	1	-1

Table 5: The motion of 7-branes and the changes of the 2-cycles along the path1.

After the step 4, A7's position and A6's position exchange with each other. Note that the A7 charge and the A6 charge are the same up to sign. Hence we do not need to rearrange the branch cuts in this exchange process. We get the Table 6 after the exchange.

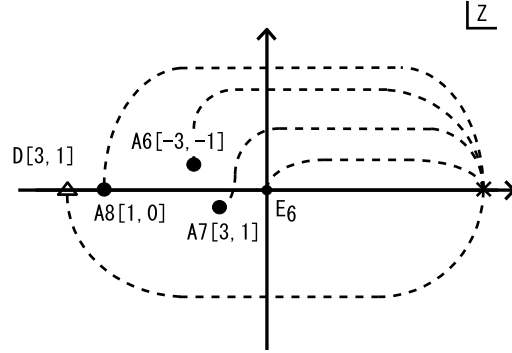


	A8[1,0]	A6[-3,-1]	A7[3,1]	A5[4,1]	A4-A1[4,1]	B[9,2]	C1, C2[-1,0]	D[3,1]
\tilde{C}_{A65}	0	1	0	-1	0	1	1	0
\tilde{C}_{A76}	0	-2	1	-1	-1	1	-1	0
\tilde{C}_{A87}	1	0	-1	1	1	-2	0	0
\tilde{C}_{BCD}	0	1	-1	1	1	-1	1	-1

Table 6: The figure shows the motion of 7-branes during the path 2 and the table represents the changes of 2-cycles after the path 2

We follow the above 4 steps backward, then we get the second part of the Table 7. The A6 charge and the A7 charge are $[-1, 0]$. Since their charge is $[1, 0]$ originally, we make their charges into the the original charges $[1, 0]$. Then the second part of the Table 7 becomes last

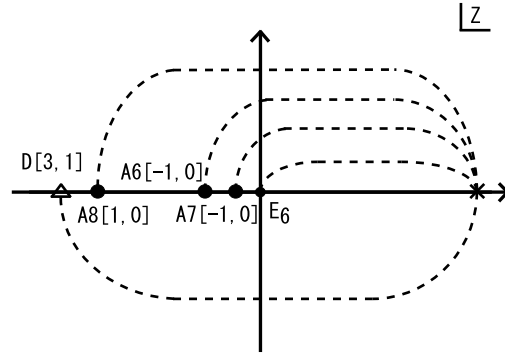
part of the Table 7.



	A8[1,0]	A6[-3,-1]	A7[3,1]	A5[4,1]	A4-A1[4,1]	B[9,2]	C1, C2[-1,0]	D[3,1]
\tilde{C}_{A65}	0	1	0	-1	0	1	1	0
\tilde{C}_{A76}	0	-2	1	-1	-1	1	-1	0
\tilde{C}_{A87}	1	0	-1	1	1	-2	0	0
\tilde{C}_{BCD}	0	1	-1	1	1	-1	1	-1

↓

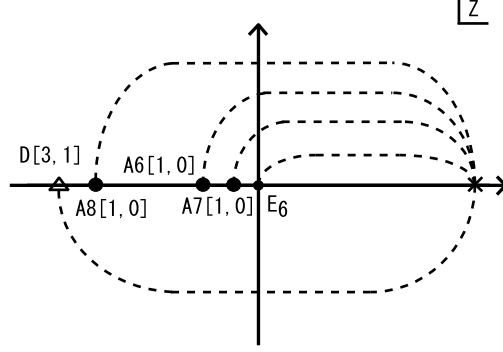
Going back the four steps of the Table 5



	A8[1,0]	A6[-1,0]	A7[-1,0]	A5[1,0]	A4-A1[1,0]	B[1,-1]	C1, C2[1,1]	D[3,1]
\tilde{C}_{A65}	0	1	1	-2	-1	4	2	0
\tilde{C}_{A76}	0	-2	-1	1	1	-4	-2	0
\tilde{C}_{A87}	1	0	-2	1	1	-4	-2	0
\tilde{C}_{BCD}	0	0	0	0	0	1	1	-1

↓

Changing the bases into the ones before the rotation



	A8[1,0]	A6[1,0]	A7[1,0]	A5[1,0]	A4-A1[1,0]	B[1,-1]	C1, C2[1,1]	D[3,1]
\tilde{C}_{A65}	0	-1	-1	-2	-1	4	2	0
\tilde{C}_{A76}	0	2	1	1	1	-4	-2	0
\tilde{C}_{A87}	1	0	2	1	1	-4	-2	0
\tilde{C}_{BCD}	0	0	0	0	0	1	1	-1

Table 7: The configurations of 7-branes and the changes of 2-cycles when we go 4 steps in the Table 5 in a backward direction. The last part shows the change of the bases into the ones at the base point.

From the first table of Table 5 and the last table of the Table 7, we get

$$\tilde{C}_{A65} = C_{-\theta} + C_{A65} + C_{A76} \quad (77)$$

$$\tilde{C}_{A76} = -C_{-\theta} \quad (78)$$

$$\tilde{C}_{-\theta} = -C_{A76} \quad (79)$$

$$\tilde{C}_{A87} = -C_{-\theta} - C_{A76} + C_{A87} . \quad (80)$$

where the equalities of the equations (77) ~ (80) should be understood up to the boundaries of the 3-dimensional cells. Note that C_α^1 , C_α^2 , C_β^1 and C_β^2 , which are the outside of E_8 are invariant. On the other hand, this monodromy acts on the 2-cycles inside E_8 as the Weyl reflection by $C_{A76} + C_{-\theta}$.

A.2.4 The monodromy of the loop γ_{0-4}

When a_0 varies along the loop γ_{0-4} , the exchange of A7 and A8 only happens (see Figure 10).

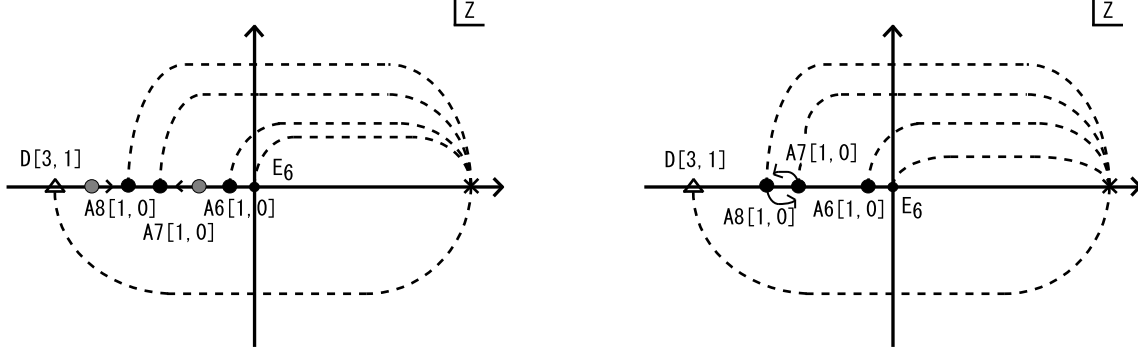


Figure 10: The left figure shows the motion of 7-branes when we approach the right of $a_0 = a_{0-4}$ singularity. The right figure shows the motion of 7-brane when we go round $a_0 = a_{0-4}$ singularity in an anti-clockwise direction.

Hence we get

$$\tilde{C}_{A76} = C_{A76} + C_{A87} \quad (81)$$

$$\tilde{C}_{A87} = -C_{A87} \quad (82)$$

$$\tilde{C}_{AA'} = -C_{A87} + C_{AA'}. \quad (83)$$

Note that C_{A87} mixes into the 2-cycles inside E_8 . This means that the monodromy of the loop γ_{0-4} causes an effect beyond E_8 gauge theory.

C_α^2 and C_β^2 do not mix with C_α^1 , C_β^1 and the 2-cycles in E_8 . We can understand this structure due to the ϵ_η scaling.

B Monodromy around $a_0 = 0$ Locus in Light of Heterotic Dual

It is instructive to see what the monodromy of 2-cycles (45–48) correspond to in Heterotic dual description. These monodromy matrices were obtained by a brute force calculation. Heterotic dual description tells us that this is a very natural result.

The duality map between F-theory and Heterotic string theory [42] is now well-understood. The moduli space of F-theory compactification on an elliptic K3 and that of Heterotic string

compactification on T^2 are both $O(2) \times O(18) \backslash O(2, 18; \mathbb{R}) / O(2, 18; \mathbb{Z})$. For the purpose of describing the action of the monodromy group $O(2, 18; \mathbb{Z})$ explicitly, however, let us begin by reminding ourselves of the basic things about the duality map, while setting up notation.

The complex structure moduli of elliptic fibered K3 manifold for F-theory compactification is described (e.g., [41]) by 20 complex numbers Π_i ($i = 1, \dots, 20$) satisfying

$$\Pi_i C^{ij} \Pi_j = 0, \quad \Pi_i C^{ij} \Pi_j^* = 2. \quad (84)$$

Multiplying an arbitrary complex phase on all the Π_i 's corresponds to the $O(2)$ redundancy of the moduli space. The moduli parameters Π_i are obtained from a defining equation of an elliptic fibered K3 manifold as period integrals

$$\Pi_i = \int_{C_i} \Omega^{(2,0)} \quad (85)$$

of a holomorphic $(2,0)$ form satisfying $\int_{K3} \Omega \wedge \bar{\Omega} = 2$. C^{ij} is the inverse matrix of the intersection form of 2-cycles of a K3 other than the zero section and the generic fiber class. We choose the first four 2-cycles to be C_α^1 , C_α^2 , C_β^1 and C_β^2 in this order, and use those in the first and last rows of Table 1 as the 16 other 2-cycles. For an elliptic fibered K3-manifold given by (11), for example,

$$\Pi_{C_\alpha^1} \sim \Pi_{C_\beta^1} \sim \frac{1}{\sqrt{\ln(1/\epsilon_\eta)}}, \quad (86)$$

$$\Pi_{C_\alpha^2} \sim \Pi_{C_\beta^2} \sim \sqrt{\ln(1/\epsilon_\eta)}, \quad (87)$$

$$\Pi_{C_{A76}} \sim \Pi_{C_{-\theta}} \sim \Pi_{C'_{-\theta}} \sim \frac{1}{\sqrt{\ln(1/\epsilon_\eta)}} \epsilon_K. \quad (88)$$

The Narain moduli of Heterotic string compactifications on a T^2 are described by 20 complex parameters

$$\Pi_i = \sqrt{\frac{\alpha'}{2}} (k_{\hat{8}R} + i k_{\hat{9}R})_i = \sqrt{\frac{\alpha'}{2}} \frac{1}{\tau_2} (-i \tau k_{8R} + i k_{9R})_i \quad (89)$$

for $i = 1, \dots, 20$; $(k_{mR})_i$ ($m = 8, 9$) above determine the momenta k_{8R} and k_{9R} in the right-moving sector by $k_{mR} = (k_{mR})_i n^i$, where $(n_i)^T$ is a charge vector

$$(n^i)^T = (n_8, -w^8, n_9, -w^9, n^{i=5, \dots, 20})^T; \quad (90)$$

(n_8, n_9) specify the Kaluza–Klein excitation level, and (w^8, w^9) are the winding numbers. $n^i \in \mathbb{Z}$'s ($i = 5, \dots, 20$) generate root lattice²⁵ of $E_8 \times E_8$. k_{8R} and k_{9R} are parametrized by 16 Wilson lines $(-i\tau A_8 + iA_9)^i \in \mathbb{C}$ ($i = 5, \dots, 20$), complex structure $\tau = \tau_1 + i\tau_2$ of the torus, R and B_{89} ; explicit expressions are found in (11.6.17) of [43].

With all the conventions fixed as above, the duality map is to identify Π_i 's of the two descriptions. One can see by comparing Π_i 's calculated on both sides that

$$\frac{R}{\sqrt{\alpha'}} \quad (\text{Het}) \leftrightarrow \sqrt{\ln(1/\epsilon_\eta)} \quad (\text{F-theory}), \quad (91)$$

as is well known [20, 27], and

$$\frac{1}{\tau_2} R(-i\tau A_8 + iA_9)^i \quad (\text{Het}) \leftrightarrow \text{fcn} \left(\frac{a_r}{a_0} \right) \sim \epsilon_K \quad (\text{F-theory}), \quad (92)$$

where we assumed that a_0 may scale as ϵ_η , but $a_{0,*}$ in (15, 16) remains $\mathcal{O}(1)$ and non-zero. Thus the choice of complex structure moduli with a small ϵ_K in (15) and $a_{0,*} \sim \mathcal{O}(1)$ in F-theory corresponds to Wilson lines in Heterotic string theory in T^2 that are parametrically smaller than the Kaluza–Klein scale of the T^2 compactification. Thus, the T^2 Kaluza–Klein states decouple and a gauge theory on $7+1$ dimensions is obtained also in the Heterotic description. The “8D gauge theory region” of F-theory moduli space corresponds to 8D gauge theory on the Heterotic side.

Both F-theory compactified on an elliptic K3 manifold and Heterotic string theory compactified on T^2 have 20 U(1) vector fields on $7+1$ dimensions. The charge vector $(n^i)^T$ that appeared in (90) specifies²⁶ charges of an object under these 20 U(1) vector fields. In the convention we adopted above, the last 16 U(1) vector fields are those in $E_8 \times E_8$. In Heterotic string compactifications, the vector fields corresponding to the charges $n_{8,9}$ are Kaluza–Klein vector fields from the metric on $9+1$ dimensions, and those to $w^{8,9}$ are those from the B -field. The monodromy group $O(2, 18; \mathbb{Z})$ acts from the right on all of 2-cycles (C_i) , moduli parameters (Π_i) , and on 20 independent U(1) vector fields.

Having prepared all above, we are now ready to interpret the monodromy matrix (45) in Heterotic dual description. Since we considered monodromy in F-theory that appears even

²⁵One can use a basis so that the last 16×16 part of the inverse of the intersection form is just a unit matrix. The last 16 components of the charge vector in this basis, n^I ($I = 5, \dots, 20$), and n^i ($i = 5, \dots, 20$) that we use in the main text, are related by $n^I = q_i^I n^i$; integer valued q_i^I 's specify the roots of E_8 corresponding to C_i .

²⁶In F-theory (M-theory is more appropriate, though), such an object corresponds to an M2-brane wrapped on a 2-cycle $C_i n^i$.

in $|\epsilon_\eta| \ll 1$, it must be a monodromy in Heterotic string theory that appear even in $R/\sqrt{\alpha'}$, that is, in a region of moduli space where supergravity + super Yang–Mill approximation can be used. In particular, the compactification can be described in terms of Calabi–Yau 3-fold and a stable vector bundle on it. The bundle is described by a spectral surface. The spectral surface in the Heterotic dual [27, 44] is given by [45, 23, 2, 24, 4]

$$a_0 + a_2x + a_3y + \cdots = 0, \quad (93)$$

using the same coefficients $a_{0,2,3,\dots}$ as in F-theory compactifications.²⁷ (x, y) are the coordinates of the elliptic fiber for the Heterotic string compactification. When $a_0 \neq 0$ and $a_r/a_0 \sim \epsilon_K^r$ for $r = 2, 3, \dots$, the spectral surface is near the zero section. In a neighbourhood of a base manifold where a_0 becomes zero, however, two roots of (93) move away from the zero section, and behave as specified by (9), which indicates that a Weyl reflection takes place within E_8 .

Noting that the monodromy matrix (46) can be decomposed into

$$\left(\begin{array}{c|c|c} 1 & & \\ \hline & -1 & -1 \\ \hline & 2 & 1 \quad 1 \\ & & 1 \\ \hline & & \mathbf{1}_{2 \times 2} \end{array} \right) = \left(\begin{array}{c|c|c} 1 & & \\ \hline & -1 & \\ \hline & 1 & \\ & & 1 \\ \hline & & \mathbf{1}_{2 \times 2} \end{array} \right) \left(\begin{array}{c|c|c} 1 & & \\ \hline & 1 & 1 \\ \hline & 2 & 1 \quad 1 \\ & & 1 \\ \hline & & \mathbf{1}_{2 \times 2} \end{array} \right); \quad (94)$$

here, we used a basis $(2C_{A76} + C_{-\theta}, C_{-\theta}, C_\alpha^1, C_\alpha^2, C_\beta^1, C_\beta^2)$, changing the first element of the basis from C_{A76} , so that the first two elements of this basis are dual to the Cartan elements $\text{diag}(2, -1, -1)$ and $\text{diag}(0, 1, -1)$ acting on $(C_{A65}, C_{A76} + C_{A65}, C_{-\theta} + C_{A76} + C_{A65})$. The first matrix on the right hand side is $W_{C_{-\theta}}$, a Weyl reflection in E_8 .

The second matrix above is not hard to understand, either. It is satisfactory that non-winding states ($w^{8,9} = 0$) remain non-winding states; since we have chosen $|\epsilon_\eta| \ll 1$ and hence $R/\sqrt{\alpha'} \gg 1$, supergravity / super Yang–Mills modes on 9+1 dimensions should not mix with winding states. When we take $|\epsilon_K| \ll 1$, the spectral surface scan the elliptic fiber once near a zero locus²⁸ of a_0 . This means that the Wilson line associated with the Weyl reflection varies by of order the Kaluza–Klein scale (i.e., $R(A_{\hat{8}} + iA_{\hat{9}})^I$ changes by $\mathcal{O}(1)$). This

²⁷The overall normalization of $a_{0,2,3,\dots}$ and $a''_{0,2,3,\dots}$ carries information— ϵ_η —in F-theory compactifications, but this information are ignored in the defining equation of the spectral surface (93) in Heterotic string, as this information is now carried by the volume of T^2 fiber R^2/α' .

²⁸This is very natural because the n -fold spectral cover given by (93) belongs to a topological class $|nK_S + \eta|$, and $a_0 \in \Gamma(S; \mathcal{O}(\eta))$.

Wilson line is identified with the original one modulo gauge transformation whose parameter depends on the T^2 direction. Thus, the Kaluza–Klein excitation number n_8 (the 3rd row) becomes $\tilde{n}_8 = n_8 + 2n^{-\theta}$ in this monodromy matrix. Once this coefficient 2 is fixed, then there is no freedom left in the 4th column, because the intersection form needs to remain invariant.

This monodromy involves field identification modulo gauge transformation depending on the T^2 direction; there is no way describing this phenomenon in a gauge theory on $7+1$ dimensions! This intuitive understanding of the monodromy matrix also explains why some $U(1)$ symmetry charges within E_8 mix up with $U(1)$ symmetries of Kaluza–Klein vector fields.

One would not bother about all these things when one considers, say, a Heterotic string compactification on a Calabi–Yau 3-fold with a vector bundle whose structure group is $SU(5)_{\text{str}}$. All the four $U(1)$ ’s in the Cartan of $SU(5)_{\text{str}}$ are broken completely, because of the ramification behavior of the spectral surface. All the four Kaluza–Klein vector fields from metric and B -field in $7+1$ dimensions do not remain in the massless spectrum in $3+1$ dimensions. Since none of those $U(1)$ vector fields and $U(1)$ symmetries available at microscopic level is relevant to low-energy physics, nobody cares how they are mixed up.

In the factorized spectral surface scenario in the context of dimension-4 proton decay problem, however, one wants to keep a $U(1)$ symmetry out of a four independent $U(1)$ ’s in $SU(5)_{\text{str}}$. For this purpose, one has to make sure that at least one $U(1)$ symmetry survives the monodromy that would potentially mix up all of $U(1)$ ’s in E_8 as well as those associated with Kaluza–Klein vector fields.

References

- [1] S. Katz and C. Vafa, “Matter From Geometry,” Nucl. Phys. B **497**, 146 (1997) [arXiv:hep-th/9606086].
- [2] R. Donagi and M. Wijnholt, “Model Building with F-Theory,” arXiv:0802.2969 [hep-th].
- [3] C. Beasley, J. J. Heckman and C. Vafa, “GUTs and Exceptional Branes in F-theory - I,” JHEP **0901**, 058 (2009) [arXiv:0802.3391 [hep-th]].
- [4] H. Hayashi, T. Kawano, R. Tatar and T. Watari, “Codimension-3 Singularities and Yukawa Couplings in F-theory,” Nucl. Phys. B **823**, 47 (2009) [arXiv:0901.4941 [hep-th]].

- [5] R. Donagi and M. Wijnholt, “Higgs Bundles and UV Completion in F-Theory,” arXiv:0904.1218 [hep-th].
- [6] R. Tatar, Y. Tsuchiya and T. Watari, “Right-handed Neutrinos in F-theory Compactifications,” Nucl. Phys. B **823**, 1 (2009) [arXiv:0905.2289 [hep-th]].
- [7] S. Cecotti, M. C. N. Cheng, J. J. Heckman and C. Vafa, “Yukawa Couplings in F-theory and Non-Commutative Geometry,” arXiv:0910.0477 [hep-th].
- [8] J. P. Conlon and E. Palti, “Aspects of Flavour and Supersymmetry in F-theory GUTs,” JHEP **1001**, 029 (2010) [arXiv:0910.2413 [hep-th]].
- [9] Appendix of [31].
- [10] R. Tatar and T. Watari, “Proton decay, Yukawa couplings and underlying gauge symmetry in string theory,” Nucl. Phys. B **747**, 212 (2006) [arXiv:hep-th/0602238].
- [11] J. Marsano, N. Saulina and S. Schafer-Nameki, “Monodromies, Fluxes, and Compact Three-Generation F-theory GUTs,” JHEP **0908**, 046 (2009) [arXiv:0906.4672 [hep-th]].
- [12] C. Beasley, J. J. Heckman and C. Vafa, “GUTs and Exceptional Branes in F-theory - II: Experimental Predictions,” JHEP **0901**, 059 (2009) arXiv:0806.0102 [hep-th].
- [13] R. Donagi and M. Wijnholt, “Breaking GUT Groups in F-Theory,” arXiv:0808.2223 [hep-th].
- [14] V. Bouchard, J. J. Heckman, J. Seo and C. Vafa, “F-theory and Neutrinos: Kaluza-Klein Dilution of Flavor Hierarchy,” JHEP **1001**, 061 (2010) [arXiv:0904.1419 [hep-ph]].
- [15] J. J. Heckman, A. Tavanfar and C. Vafa, “The Point of E_8 in F-theory GUTs,” arXiv:0906.0581 [hep-th].
- [16] R. Blumenhagen, T. W. Grimm, B. Jurke and T. Weigand, “Global F-theory GUTs,” Nucl. Phys. B **829**, 325 (2010) [arXiv:0908.1784 [hep-th]].
- [17] O. DeWolfe, T. Hauer, A. Iqbal and B. Zwiebach, “Uncovering infinite symmetries on (p,q) 7-branes: Kac-Moody algebras and beyond,” Adv. Theor. Math. Phys. **3**, 1835 (1999) [arXiv:hep-th/9812209].
- [18] M. Bershadsky, K. A. Intriligator, S. Kachru, D. R. Morrison, V. Sadov and C. Vafa, “Geometric singularities and enhanced gauge symmetries,” Nucl. Phys. B **481**, 215 (1996) [arXiv:hep-th/9605200].
- [19] S. Katz and D. R. Morrison, “Gorenstein Threefold Singularities with Small Resolutions via Invariant Theory for Weyl Groups,” J. Alg. Geom. **1** (1992) 449–530 [arXiv:alg-geom/9202002].

- [20] D. R. Morrison and C. Vafa, “Compactifications of F-Theory on Calabi–Yau Threefolds – II,” Nucl. Phys. B **476**, 437 (1996) [arXiv:hep-th/9603161].
- [21] K. Dasgupta, G. Rajesh and S. Sethi, “M Theory, Orientifolds and G-Flux,” JHEP **9908**, 023 (1999) [arXiv:hep-th/9908088].
- [22] F. Cachazo, S. Katz and C. Vafa, “Geometric transitions and $N = 1$ quiver theories,” arXiv:hep-th/0108120.
- [23] G. Curio and R. Y. Donagi, “Moduli in $N = 1$ heterotic/F-theory duality,” Nucl. Phys. B **518** (1998) 603 [arXiv:hep-th/9801057].
- [24] H. Hayashi, R. Tatar, Y. Toda, T. Watari and M. Yamazaki, “New Aspects of Heterotic–F Theory Duality,” Nucl. Phys. B **806**, 224 (2009) [arXiv:0805.1057 [hep-th]].
- [25] A. Johansen, “A comment on BPS states in F-theory in 8 dimensions,” Phys. Lett. B **395**, 36 (1997) [arXiv:hep-th/9608186].
- [26] M. R. Gaberdiel and B. Zwiebach, “Exceptional groups from open strings,” Nucl. Phys. B **518**, 151 (1998) [arXiv:hep-th/9709013].
- [27] R. Friedman, J. Morgan and E. Witten, “Vector bundles and F theory,” Commun. Math. Phys. **187** (1997) 679 [arXiv:hep-th/9701162].
- [28] J. Marsano, N. Saulina and S. Schafer-Nameki, “F-theory Compactifications for Supersymmetric GUTs,” JHEP **0908**, 030 (2009) [arXiv:0904.3932 [hep-th]].
- [29] O. DeWolfe and B. Zwiebach, “String junctions for arbitrary Lie algebra representations,” Nucl. Phys. B **541**, 509 (1999) [arXiv:hep-th/9804210];
O. DeWolfe, T. Hauer, A. Iqbal and B. Zwiebach, “Uncovering the symmetries on (p,q) 7-branes: Beyond the Kodaira classification,” Adv. Theor. Math. Phys. **3**, 1785 (1999) [arXiv:hep-th/9812028].
- [30] A. Klemm, B. Lian, S. S. Roan and S. T. Yau, “Calabi-Yau fourfolds for M- and F-theory compactifications,” Nucl. Phys. B **518**, 515 (1998) [arXiv:hep-th/9701023].
- [31] H. Hayashi, T. Kawano, Y. Tsuchiya and T. Watari, “Flavor Structure in F-theory Compactifications,” arXiv:0910.2762 [hep-th].
- [32] C. Cordova, “Decoupling Gravity in F-Theory,” arXiv:0910.2955 [hep-th].
- [33] J. J. Heckman and C. Vafa, “Flavor Hierarchy From F-theory,” arXiv:0811.2417 v2 [hep-th].

- [34] F. Marchesano and L. Martucci, “Non-perturbative effects on seven-brane Yukawa couplings,” arXiv:0910.5496 [hep-th].
- [35] A. Font and L. E. Ibanez, “Matter wave functions and Yukawa couplings in F-theory Grand Unification,” JHEP **0909**, 036 (2009) [arXiv:0907.4895 [hep-th]].
- [36] C. M. Chen and Y. C. Chung, “A Note on Local GUT Models in F-Theory,” Nucl. Phys. B **824**, 273 (2010) [arXiv:0903.3009 [hep-th]];
Y. C. Chung, “Abelian Gauge Fluxes and Local Models in F-Theory,” JHEP **1003**, 006 (2010) [arXiv:0911.0427 [hep-th]].
- [37] J. L. Bourjaily, “Local Models in F-Theory and M-Theory with Three Generations,” arXiv:0901.3785 [hep-th].
- [38] F. Denef, “Les Houches Lectures on Constructing String Vacua,” arXiv:0803.1194 [hep-th].
- [39] J. H. Schwarz, “From Superstrings to M Theory,” Phys. Rept. **315** (1999) 107 [arXiv:hep-th/9807135].
- [40] M. R. Gaberdiel, T. Hauer and B. Zwiebach, “Open string-string junction transitions,” Nucl. Phys. B **525**, 117 (1998) [arXiv:hep-th/9801205].
- [41] P. S. Aspinwall, “K3 Surfaces and String Duality,” arXiv:hep-th/9611137.
- [42] C. Vafa, “Evidence for F-Theory,” Nucl. Phys. B **469**, 403 (1996) [arXiv:hep-th/9602022].
- [43] J. Polchinski, “*String Theory*,” Cambridge (1998).
- [44] R. Donagi, “Principal bundles on elliptic fibrations,” Asian. J. Math **1** (1997) 214 [arXiv:alg-geom/9702002];
R. Donagi, “Taniguchi lecture on principal bundles on elliptic fibrations,” arXiv:hep-th/9802094.
- [45] S. Katz, P. Mayr and C. Vafa, “Mirror symmetry and exact solution of 4D $N = 2$ gauge theories. I,” Adv. Theor. Math. Phys. **1**, 53 (1998) [arXiv:hep-th/9706110];
P. Berglund and P. Mayr, “Heterotic string/F-theory duality from mirror symmetry,” Adv. Theor. Math. Phys. **2**, 1307 (1999) [arXiv:hep-th/9811217].